T-1553

FILM BOILING HEAT TRANSFER BETWEEN CRYOGENIC LIQUIDS AND WATER

By

Charles R. Vesta]

7576/36

T-1553

A dissertation submitted to the Faculty and the Board of Trustees of the Colorado School of Mines in partial fulfillment of the requirements for the degree of Doctor of Philosophy in Chemical and Petroleum-Refining Engineering.

Signed: Charles R. Jeutal
Student

Golden, Colorado
Date: October 31 1973

Approved: P. F. Dickson
Advisor

P. F. Dickson
Head of Department

Golden, Colorado
Date: October 31, 1973

ABSTRACT

Transient interfacial heat fluxes and interfacial heat transfer coefficients have been experimentally determined as functions of the interfacial temperature difference for liquid nitrogen, liquid methane gas, and liquid natural gas film boiling on water. Interfacial heat flux ranges from 0.5-2.1 cal/cm^2-sec for liquid nitrogen-water at interfacial temperature differences of 210-256°K, 1.0-4.7 cal/cm^2-sec for liquid methane-water at interfacial temperature differences of 188-220°K, and 3.0-13.1 cal/cm^2-sec for liquid natural gas-water at interfacial temperature differences of 188-220°K. Corresponding interfacial heat transfer coefficients range from 0.0024-0.0082 cal/cm^2-sec-°K for liquid nitrogen-water, 0.0053-0.0241 cal/cm^2-sec-°K for liquid methane-water, and 0.0163-0.0653 cal/cm^2-sec-°K for liquid natural gas-water. Estimated experimental error is ±13.3%.

The experimental equipment used in this investigation consists of a glass dewar flask mounted on a load cell and equipped with a thermocouple temperature measuring system. Water is contained in the experimental dewar and the cryogenic liquid is poured onto the surface. The load cell continuously records the vaporization rate of the cryogenic liquid

which is a direct measure of the interfacial heat flux. Thermocouples measure the surface temperature of the water layer, temperatures within the water layer, and the temperature of the boiling cryogenic liquid.

Insufficient data were obtained in this study to develop a generalized mathematical correlation describing the film boiling of cryogenic liquids on water. Additional work, both experimental and theoretical, needs to be undertaken in this area.

ACKNOWLEDGMENTS

Research and academic work resulting in the completion of a dissertation and graduate study program for a part-time student is the culmination of the efforts of many different individuals. The author is deeply indebted to numerous individuals for aid and assistance which made this work possible.

This investigation was undertaken under the guidance of Dr. P. F. Dickson, Head, Chemical and Petroleum-Refining Engineering Department, to whom the author wishes to extend his sincere thanks for all of the encouragement, advice, and guidance he provided.

Thanks are due to Dr. A. J. Kidnay, Chemical and Petroleum-Refining Engineering Department, and Dr. R. E. D. Woolsey, Mathematics Department, for their assistance and teaching.

Special acknowledgment is made of the support provided by the management and staff of the Denver Research Center, Marathon Oil Company, who provided laboratory space, experimental equipment, and cryogenic materials. The author would like to thank each of the individuals who contributed to and encouraged work on this investigation.

Lastly, I wish to acknowledge the special support and encouragement provided by my family. No words can adequately express my thanks for the special assistance and sacrifices they made for me. Without the help of my wife, Madelene, my graduate studies would never have been successfully completed. This dissertation is lovingly dedicated to her.

TABLE OF CONTENTS

FIGURES

TABLES

INTRODUCTION

The problem of boiling heat transfer between two immiscible liquids has recently been encountered in studies of spills of cryogenic liquids onto water. Stringent safety precautions associated with the marine transportation of liquid natural gas (LNG) and other liquefied gases have raised questions regarding what potential problems exist should a spill occur. One of the principal questions is to determine the rate at which heat is transferred across the liquid cryogen-water interface.

Ideally, the transfer of heat can be compared with the transfer of electric current: a potential or driving force acting through a resistance causes a transport of current. In the case of heat transfer, the potential is a temperature difference, and the current a heat flux. The resistance is referred to as the heat transfer coefficient. The purpose of this investigation is to experimentally determine the interfacial heat transfer coefficient for a cryogenic liquid film boiling on a water surface.

Film boiling between two immiscible liquids is a mode of heat transfer where the generation of vapor from the volatile phase occurs so rapidly that a stable film of vapor separates the two liquids. This is the

case for cryogenic liquids spilled on water because of the large temperature difference which exists.

Cryogenic liquids used in this investigation are liquid nitrogen, liquid methane, liquid ethane, liquid propane, and liquid natural gas. These materials were chosen for study since they are presently being transported in large quantities.

Experimentally, the scope of this study is limited to the transient boiling of a cryogenic liquid on a liquid water surface at atmospheric pressure. The freezing and boiling points of the water layer limit the range of possible temperatures available in the water layer. The range of interfacial temperature differences available for study is then controlled by the normal boiling point of the cryogenic liquid.

LITERATURE REVIEW

An extensive literature search has been made in the area of film boiling of cryogen liquids on water. Published work in this area is minimal. A qualitative overview of the experimental work in dealing with spills of cryogens on water is given by Nakanishi (1971a, p. 37). This paper discusses a number of qualitative experiments aimed at determining the behavior of boiling liquids on the surface of other liquids.

A discussion of the quantitative experiments, observations, and experimental data which have been reported will follow. This discussion will present the published results in the chronological order in which they were conducted.

Burgess (1970, p. 4) performed early experiments in this area. A 60- by 30- by 30-cm aquarium containing 20 l of water was used in all experiments. Liquid nitrogen (LN_2) and liquid natural gas (LNG) were spilled onto the water surface. The aquarium was positioned on a load-cell in order to obtain vaporization rates of the cryogenic liquids. An array of thermocouples positioned near the water surface was also used. Significant results and observations are as follows:

1) The LN_2-water interface was violently agitated; however, the LNG-water interface was relatively quiet.

2) An ice film which completely covered the surface of the water formed in the LN_2 spillage tests after about 10 sec. In the LNG-water tests ice formed in approximately 2-3 sec.

3) Spills of LNG on water produced considerable foaming.

4) Spills on water, ice, and brine (3% NaCl solution) produced similar results. An average heat flux of 2.5 ± 0.25 cal/cm^2-sec (33,000 ± 3,400 Btu/ft^2-hr) was reported for LNG, and a heat flux of 0.6 ± 0.2 cal/cm^2-sec (8,000 ± 2,300 Btu/ft^2-hr) was reported for LN_2. In the analysis of the experimental data the vaporization rate was averaged over a 20-sec time period.

5) The thermocouple array positioned at the water interface did not provide any usable information. A thermocouple positioned 5 mm below the surface showed that after approximately 15 sec, the temperature dropped from the initial value of 320°K to the freezing point of water (273.1°K), and then dropped to approximately 144°K after 60 sec.

6) Quantities of LN_2 and LNG used in the experiments ranged from 2,000-3,200 g. Depth of the cryogenic liquid on the water surface was nominally 4.3 cm.

Nakanishi (1971b, p. 1) conducted experiments to measure the boiling heat fluxes for LN_2, condensed pipeline natural gas (CPG), liquid methane gas (LMG), and liquid ethane gas (LEG) on water. The experimental apparatus used was very simple. A 120 mm ID unsilvered dewar flask mounted

on a load-cell was equipped with a set of thermocouples to measure the water layer temperature. Thermocouples were fabricated from 24 gage (0.51 mm OD) bare copper-constantan wire. These thermocouples were installed from the top of the dewar test vessel so that they had to pass through the boiling cryogenic liquid and the cryogen-water interface. In all tests the boiling cryogen completely covered the water surface. Significant results for the systems studied are given below.

1) When LN_2 was poured on water at a temperature of 278°K, an ice layer formed in about 10 sec, and a constant boiling heat flux of approximately 0.75 cal/cm^2-sec (10,000 Btu/ft^2-hr) was observed throughout the experimental run. Water temperature measured 5 mm below the surface dropped to nearly 105°K after 90 sec.

2) When LN_2 was spilled on water at a temperature of 353°K, no ice layer formed during the experimental run. Heat fluxes reported for this experiment decreased as the experiment progressed. The following table summarizes the data.

TABLE 1

BOILING HEAT FLUX LN_2-WATER SYSTEM

(Nakanishi, 1971b, p. 1)

Initial Water Temperature: 353°K

Time, sec	Heat Flux	
	cal/cm^2-sec	Btu/ft^2-hr
10	2.0	26,500
20	1.6	21,000
30	1.2	16,000
40	1.0	13,000
50	0.9	11,500
60	0.7	9,000

3) Condensed pipeline natural gas (CPG) was poured on water surfaces maintained at 273, 278, 293, 323, and 353°K. At the first three water temperature levels ice formed on the surface within a few seconds; no ice formed in the latter two runs. Analysis of the CPG is given in Nakanishi (1971a, p. 38) as 4.3 mole % nitrogen and 95.7 mole % methane.

4) Heat fluxes reported for the CPG-water experiments decreased as the experiment progressed. Other details were also given:

a) Boiling heat flux during the first 10 sec of the experimental run was reported a maximum of 5.7 cal/cm^2-sec (75,000 Btu/ft^2-hr) on 353°K water and a minimum of 4.4 cal/cm^2-sec (59,000 Btu/ft^2-hr) on 323°K water. Water temperatures of 273, 278, and 293°K gave intermediate values for the boiling heat flux.

b) The rate at which the boiling heat flux decreased is shown in the following table:

TABLE 2

BOILING HEAT FLUX CPG-WATER SYSTEM

(Nakanishi, 1971b, p. 2)

Initial Water Temperature: 353°K

	Heat Flux	
Time, sec	cal/cm^2-sec	Btu/ft^2-hr
10	5.7	75,500
20	4.7	62,000
30	3.4	45,000

c) When the initial water temperature was either 273 or 278°K, the temperature measured 5 mm below the interface dropped to approximately 195°K within 45 sec. The boiling point of the CPG was reported to be approximately 111°K and to remain constant throughout the run.

5) Liquid methane gas (LMG) was spilled on water at a temperature of 278°K in one run. Boiling heat flux is given in the following table:

TABLE 3

BOILING HEAT FLUX LMG-WATER SYSTEM

(Nakanishi, 1971b, p. 3)

Initial Water Temperature: 278°K

	Heat Flux	
Time, sec	cal/cm^2-sec	Btu/ft^2-hr
10	4.7	62,000
20	3.9	52,000
30	3.4	45,000
40	3.0	40,000
50	2.8	37,500

6) Liquid ethane gas (LEG) was spilled on water at a temperature of 278°K in one run. Boiling heat flux is shown in the following table:

TABLE 4

BOILING HEAT FLUX LEG-WATER SYSTEM

(Nakanishi, 1971b, p. 4)

Initial Water Temperature: 278°K

	Heat Flux	
Time, sec	cal/cm^2-sec	Btu/ft^2-hr
10	3.3	43,000
20	2.8	37,500
30	2.5	32,500
40	2.1	28,000
50	1.9	25,000

7) Visual observations of the boiling process for LMG-water and LEG-water were not reported.

Burgess (1972, p. 9) conducted additional experiments to further analyze the heat transfer rate between LN_2-water, LMG-water and LNG-water. A polystyrene foam water container holding 6,000 g of water was used in all experiments. From 2-5 l of cryogen was poured from a height of 45 cm onto the water surface. The surface area was 742.3 cm^2. Weight loss of the cryogenic liquid was observed at 50 g intervals. No temperature measurements were made. Significant results are reported as follows:

1) For LN_2-water spills, a boiling heat flux of 0.8 ± 0.1 cal/cm^2-sec (10,450 ± 750 Btu/ft^2-hr) is reported. This value is determined from an average evaporation rate over a 20-sec time period.

2) In LMG-water systems several different results are given. These results reflect the initial quantity of LMG spilled, and the time frame within which the data are averaged. The following table summarizes the results.

TABLE 5

BOILING HEAT FLUX LMG-WATER SYSTEM

(Burgess, 1972, p. 15)

Liquid Methane Volume, l	Heat Flux			
	Avg. 0-20 sec		Avg. 30-60 sec	
	cal/cm^2-sec	Btu/ft^2-hr	cal/cm^2-sec	Btu/ft^2-hr
2.0	1.3 ± 0.05	17,500 ± 630	2.3 ± 0.2	30,040 ± 2,070
3.0	1.7 ± 0.3	22,260 ± 3,490	2.2 ± 0.2	28,940 ± 2,080
4.5	2.2 ± 0.1	29,070 ± 1,580	2.7 ± 0.1	35,350 ± 1,040

3) The reported value of boiling heat flux for LNG-water is 2.1 ± 0.2 cal/cm^2-sec (28,400 ± 2,500 Btu/ft^2-hr). An average evaporation rate over a 20-sec time period is used in the determination of the LNG-water boiling heat flux.

Published literature on the quantitative experiments give essentially the same results. The boiling heat flux for LN_2-water is less than LMG-water which is less than LNG-water. A single experimental run shows that LEG-water is slightly less than LMG-water. No interfacial heat transfer coefficients are reported in the published literature. Values for the boiling heat flux in the LN_2-water system vary from 0.6 to 2.0 cal/cm^2-sec, in the LNG-water system differences of from 2.5 to 5.7 cal/cm^2-sec are reported, and in the LMG-water system values of 1.3 to 4.7 cal/cm^2-sec are given.

INSTRUMENTATION AND EQUIPMENT

An overall schematic diagram of the experimental equipment used in this study is shown in Figure 1. A cryogenic liquid is poured onto water contained in a special dewar flask. Immediate boiling occurs due to the large temperature difference, causing the cryogen to rapidly evaporate. The rate at which this vaporization occurs is measured directly by a weight measurement system consisting of a load cell and recorder. Thermocouples are located in the water layer at various depths below the water surface. The surface temperature as well as temperature gradients in the water layer can be measured directly by these thermocouples. An additional thermocouple is used to monitor the temperature of the boiling cryogenic liquid. Different rates of heat transfer are obtained by changing the initial temperature of the water layer. Detailed descriptions of the major subsystems of the experimental equipment will be described in the following sections.

Experimental Dewar

A specially constructed glass dewar flask made by the R. H. Allen Company, Boulder, Colorado, was used in all experimental runs. This

experimental dewar is shown schematically in Figure 2. The inner cylinder of the experimental dewar consists of a 46 mm ID by 1 mm wall thickness cylinder which is 210 mm long. A standard taper 24/40 ground glass female fitting is attached to the bottom end of this cylinder. A teflon plug is machined to fit into this glass fitting to serve as the means of introducing instrumentation leads for the thermocouples in the water layer into the experimental dewar flask. The inner cylinder is supported within an outer shell. This outer shell consists of a 75 mm OD by 1.5 mm wall thickness cylinder fused to the inner cylinder at both the top and bottom. A special thermal expansion ring is formed in the outer shell to allow for rapid temperature changes caused when the cryogen is poured into the apparatus. Insulation for the experimental dewar is obtained by evacuating the space between the inner and outer cylinders. A vacuum level of 1×10^{-6} torr is obtained prior to sealing the glass pumpout connection.

Special design parameters considered in the construction of the experimental dewar include:

a) Glass construction is used throughout the experimental dewar because of its low thermal conductivity. A construction material with low thermal conductivity will reduce wall conduction and therefore minimize the wall effects on the heat transfer.

b) The inner cylinder thickness is as small as possible to reduce the sensible thermal energy stored in it and thereby reduce the wall effects.

c) A bottom opening is used for instrumentation leads so that the interface between the cryogen and the water layer will not be physically disturbed.

d) Thermal tempering of the water layer instrumentation leads is obtained by introducing them through the bottom.

e) Glass construction allows visual and photographic examination of the interface between the cryogen and the water layer as boiling is taking place.

Temperature Measurement System

A system of differential thermocouples is used to determine the surface temperature and temperature gradients in the water layer. Special calibration iron-constantan (ANSI Type J) thermocouples manufactured by the Claud S. Gordon Company, Richmond, Illinois, are constructed as shown in Figure 3. The Type J thermocouple is constructed with a positive iron wire and a negative constantan (a 55% Cu-45% Ni alloy) wire. This thermocouple is specially suited for applications involving temperatures near ambient because it has high sensitivity, i. e., large change in emf per degree of temperature change. Type J thermocouples used in this study are constructed from 38-gage (0.099 mm OD) wires contained within a 0.508 mm OD protective sheath made of 304 stainless steel. Magnesium oxide (MgO) is used as insulation within the thermocouple sheath. In order to provide fast response time, a grounded junction is used. This means that the junction of the thermocouple is welded to the protective sheath. Maximum response speed can be obtained by using an exposed measuring

junction; however, an exposed Type J thermocouple cannot be used in water because of corrosion. Maximum limits of error as reported by the manufacturer are ±1.1°K over the range 273-630°K, and the thermocouple response speed is estimated to be approximately 0.003 sec.

A differential thermocouple is also used to monitor the temperature of the boiling cryogenic liquid. A special calibration copper-constantan (ANSI Type T) thermocouple manufactured by Omega Engineering, Inc., Stamford, Connecticut, is used for this purpose. Figure 4 gives details of how the Type T thermocouple is constructed. This thermocouple is recommended for low-temperature work since the homogeneity of the component wires can be maintained better than other base metal wires. Because of this, errors due to inhomogeneity of the wires in zones of temperature gradients are greatly reduced. Physically, the Type T thermocouple is the same size as the Type J thermocouples discussed previously and is shielded with similar materials. An exposed measuring junction is used since corrosion is not a factor. Maximum limits of error as reported by the manufacturer are ±1% in the low temperature range. At the liquid nitrogen normal boiling point of 77.35°K the maximum error would be ±0.77°K. Thermocouple response speed is estimated to be approximately 0.002 sec.

Voltages developed across the differential thermocouples are measured on a Honeywell, Model 1508 Visicorder, direct-recording oscillograph manufactured by Honeywell, Test Instruments Division, Denver, Colorado. Basically, a galvanometer circuit is used in this recording

oscillograph to transfer current and voltage variations to a photographic record. In this study, the oscillograph was equipped with Honeywell, Series "M" Sub-miniature, Type M40-350A, galvanometers. In order to use this rapid recording system, the thermocouple signals are amplified in a specially designed thermocouple amplifier before being sent to the recorder. Details of the design of the thermocouple amplifier are given in Appendix II.

A special temperature controlled oven is used for the thermocouple reference junctions. An ice bath could have been used for the reference junctions; however, better control of the reference temperature as well as overall convenience are obtained with a reference oven. Details of the design of the thermocouple reference oven are given in Appendix II.

One additional consideration must be taken into account in the temperature measuring system. This is the fact that when changing from the thermocouple metal wires to the recorder a thermocouple junction can be created. This is particularly true in the case of Type J thermocouples and is shown on Figure 3 as termination junctions. To avoid any problems associated with this, all thermocouple-to-instrument junctions were maintained in an isothermal environment. The Type J thermocouples were individually calibrated throughout the temperature range 273-365°K to avoid any spurious emf problems. A final accuracy for the Type J thermocouples of ±2°K was obtained on the oscillograph record. The Type T thermocouples were checked against published emf versus temperature tables and found to be within the stated accuracy. An overall accuracy of ±2°K was obtained on the oscillograph record.

Weight Measurement System

Measurements of the rate of vaporization of the boiling cryogenic liquid are made by a load cell system. A Statham Instruments, Inc., Model UC-3, Universal Transducing Cell in conjunction with a Statham Instruments, Inc., Model UL-4, 0-5 lb load cell adapter is used to continuously record the weight of the entire experimental dewar system. Since the load cell works only in compression, the entire experimental dewar system is suspended in a metal bracket from the load cell. The thermal expansion ring in the outer shell of the glass dewar flask serves as a convenient means of attaching the metal suspension bracket. Figure 5 shows how an external electrical system has been added to the load cell to allow for zeroing out the tare weight of the experimental dewar system. In practice, the zero balance potentiometer is adjusted to give a null signal with the water layer at the desired level. As the cryogenic liquid is poured onto the water surface, a positive output is obtained from the load cell. A signal of approximately 1 mv is obtained for a weight increase of 50 g. The signal from the transducer is passed through a signal conditioner and routed to the direct-recording oscillograph. A sensitivity of ±0.1 g is obtained from the load cell system. Design information for the load cell signal conditioner is given in Appendix II.

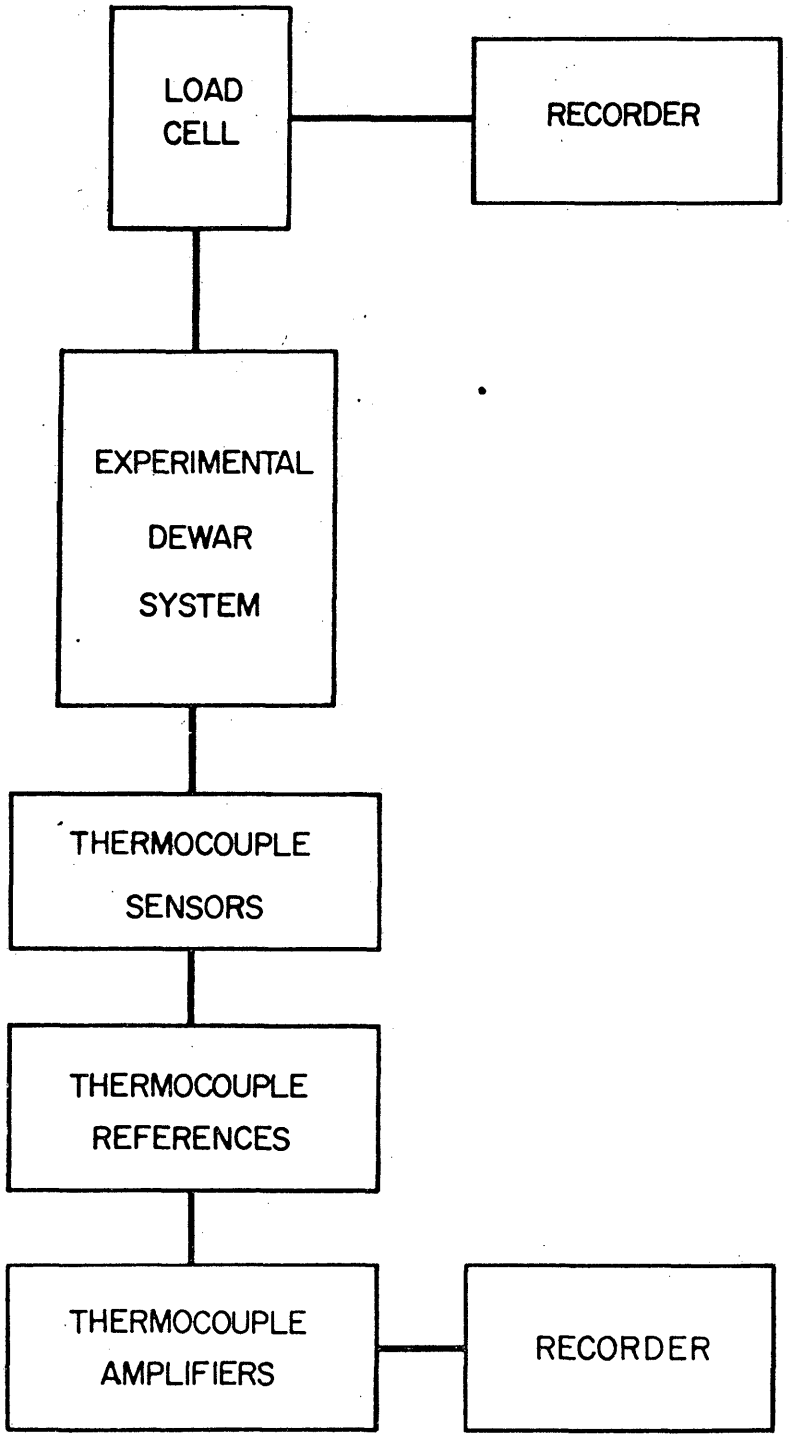

FIGURE 1. SCHEMATIC BLOCK DIAGRAM OF EXPERIMENTAL EQUIPMENT

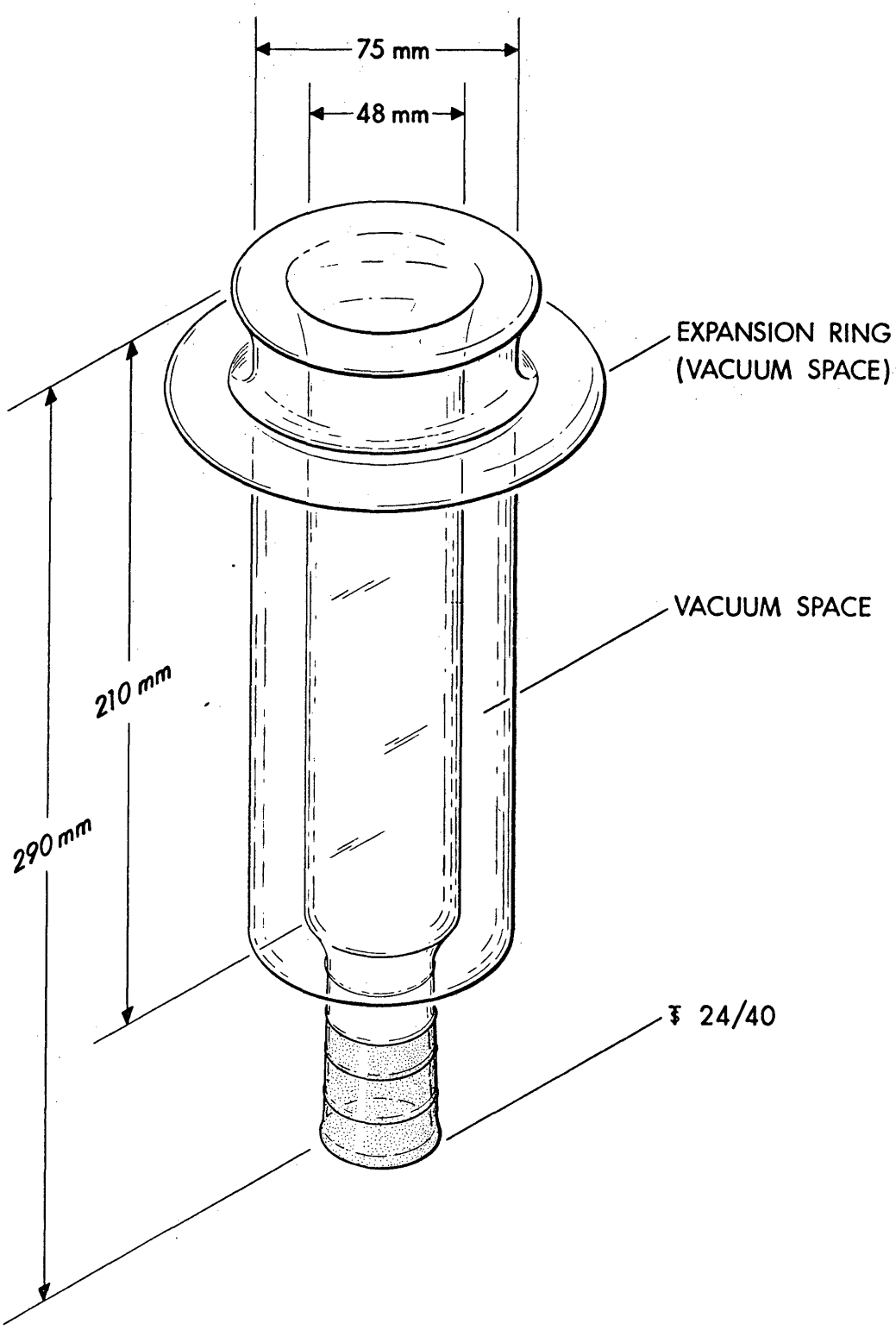

FIGURE 2. SCHEMATIC DIAGRAM OF EXPERIMENTAL DEWAR FLASK

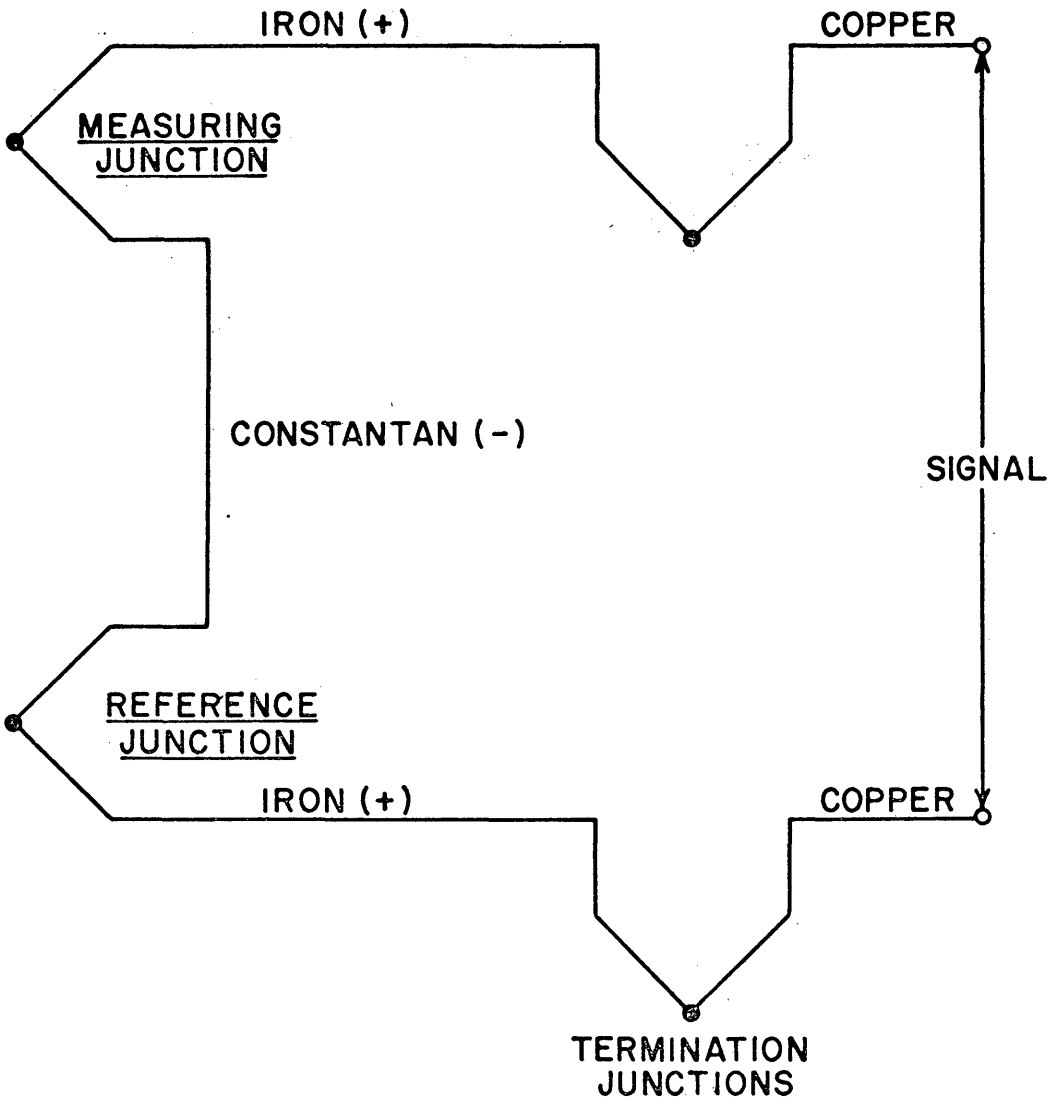

FIGURE 3. DETAILS OF DIFFERENTIAL THERMOCOUPLE CONSTRUCTION TYPE J THERMOCOUPLE

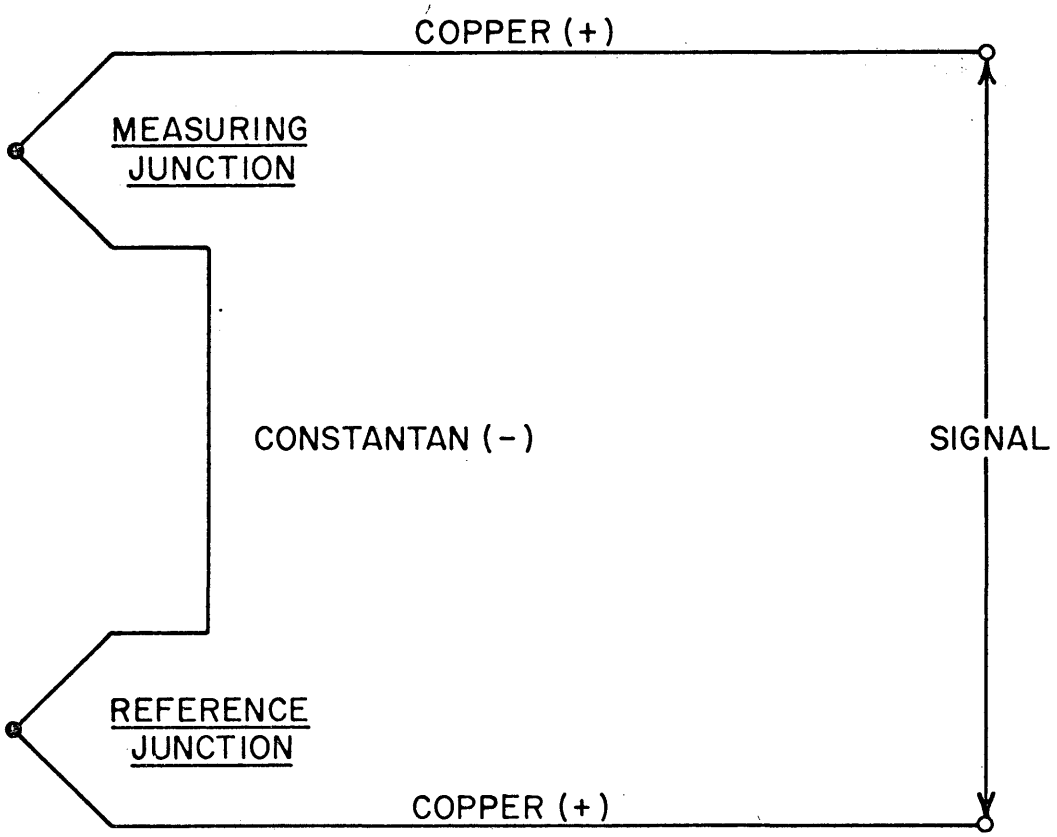

FIGURE 4. DETAILS OF DIFFERENTIAL THERMOCOUPLE CONSTRUCTION TYPE T THERMOCOUPLE

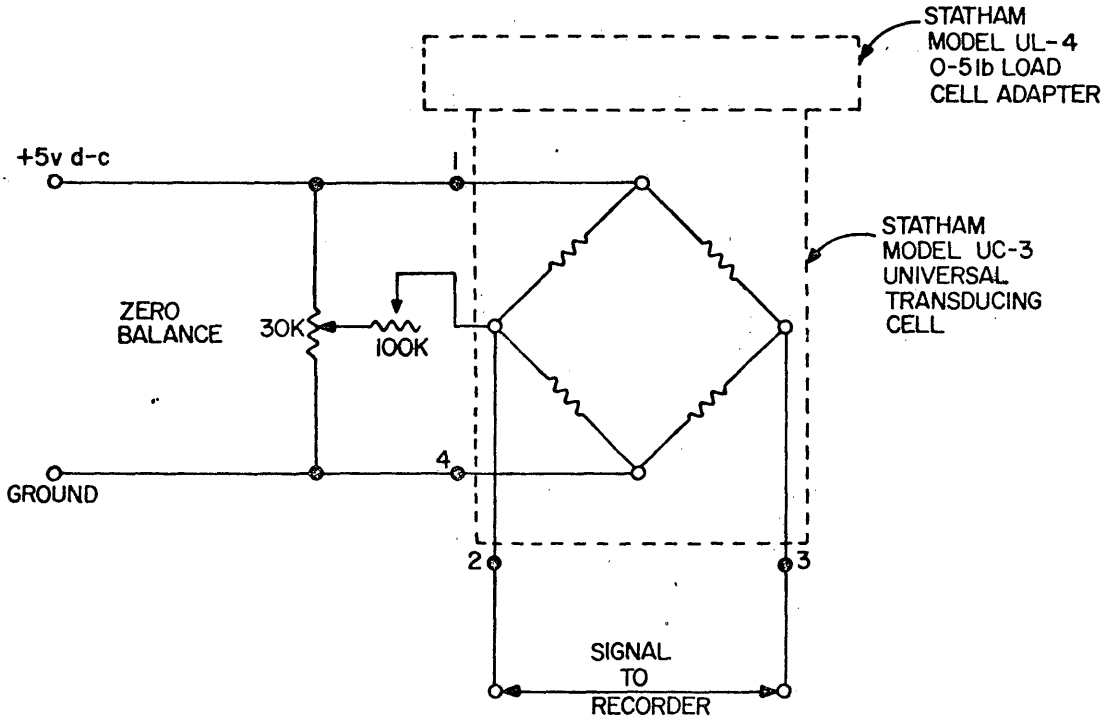

FIGURE 5. SCHEMATIC DIAGRAM OF LOAD CELL CIRCUIT

EXPERIMENTAL PROCEDURES

Procedures followed in this study to obtain the basic experimental data and to calculate the experimental results will be discussed in the following sections. Each section will be presented in the same order as the experiment was conducted.

Preparing the Water

Water which has been distilled, deionized, deoxygenated by boiling, and filtered is used in all experimental runs. The reason for the extensive preparation of the water used in this study is to be able to insure reproducibility of the water interface. Exactly 100.0 g of water is added to the experimental dewar. During the initial equipment setup, 100.0 g of water is charged to the experimental dewar and the zero balance potentiometer is adjusted to give a null output signal. The Type J thermocouples are now positioned at the desired levels in the water layer. One thermocouple is located at the lower surface of the interface, one located 10 mm below and another 30 mm below the interface. Figure 6 shows details of how the thermocouples are initially positioned at a greater depth and how the addition of the cryogenic liquid depresses the surface

to the desired level. Once this initialization has been established, the addition of 100.0 g of water to the experimental dewar is easily made.

Water in the experimental dewar is used for one experiment only. Water is heated approximately 5°K above the desired level prior to adding it to the experimental dewar. Cooling occurs as the experimental dewar is heated by the water. Approximately 15 min is allowed for this thermal equilibrium to occur.

Preparing the Cryogenic Liquid

Five different cryogenic liquids were used in this study. They were liquid nitrogen gas (LN_2), liquid methane gas (LMG), liquid natural gas (LNG), liquid ethane gas (LEG), and liquid propane gas (LPG). Each of the cryogenic liquids was contained in a storage dewar at its normal boiling point prior to use in the experiment.

Liquid nitrogen gas (LN_2) was purchased from Empire Welding Co., Denver, Colorado, for use in experiments as well as for use in condensing and liquefying the other gases. Purity of the LN_2 is 99.0 mole %.

Methane, ethane, and propane gases were obtained from Phillips Petroleum Company, Bartlesville, Oklahoma, and were liquefied and used in the experiments. Purity of the materials is 99.0 mole %.

The liquid natural gas (LNG) was obtained by condensing city pipeline gas. An exact analysis of this LNG is not available because of difficulties in sampling. An approximate analysis (via gas chromatography) is given in the following table.

TABLE 6

LIQUID NATURAL GAS ANALYSIS

Component	Mole %
Nitrogen	0.55
Methane	92.58
Ethane	6.27
Propane	0.40
Balance	0.20
	100.00

This LNG had an initial boiling point of 108.5°K immediately after liquefaction. The boiling point slowly increased as the LNG was maintained in the storage dewar.

Taking the Data

In this study, the basic data were obtained experimentally as follows:

1) Record atmospheric pressure and initial temperature of the water layer.

2) Transfer approximately 40 g of the cryogenic liquid from the storage dewar to a 50 cc glass dewar. Measure the normal boiling point of the cryogenic liquid.

3) Start the chart on the direct-recording oscillograph. Because rapid transients are expected, a chart speed of 50.8 cm/min is used.

4) Rapidly pour the cryogenic liquid onto the water surface. This should take no longer than 1 sec.

5) Visually observe the initial transient phenomena which are occurring. This includes immediate formation of ice around the perimeter

of the experimental dewar above the water interface, foaming and rapid boiling due to sensible heat stored in the walls of the experimental dewar, as well as sloshing and splashing of the cryogenic liquid due to the pouring action.

6) After the initial transients have diminished, indicate on the recorder chart that data is being taken which is usable.

7) Stop taking data when either ice forms at the interface or the complete surface of the water is not completely covered with cryogenic liquid.

Calculating the Results

Instantaneous heat transfer coefficients are calculated from an interfacial energy balance. In the boiling cryogenic liquid, the energy transferred appears in the vaporization of the liquid.

$$q = -\Delta H_v \frac{dm}{dt} \tag{1}$$

where q = rate of energy flow across a surface, cal/sec

ΔH_v = latent heat of vaporization, cal/g

$\frac{dm}{dt}$ = change in mass per unit time, g/sec

The total energy transferred is assumed to come from the water layer only. Effects of free convection, radiation, and energy entering through the experimental dewar side wall are neglected.

The heat transfer coefficient is defined by

$$q = h_i A_i \Delta T \tag{2}$$

where h_i = interfacial heat transfer coefficient, cal/cm^2-sec-°K

A_i = interfacial area, cm^2

ΔT = temperature difference, °K

The temperature difference is defined by

$$\Delta T = T_{ws} - T_c \tag{3}$$

where T_{ws} = temperature of the water surface, °K

T_c = temperature of the cryogenic liquid, °K

Combining Equations (1), (2), and (3)

$$-\Delta H_v \frac{dm}{dt} = h_i A_i (T_{ws} - T_c) \tag{4}$$

rearranging

$$h_i = \frac{-\Delta H_v \frac{dm}{dt}}{A_i (T_{ws} - T_c)} \tag{5}$$

Additionally, Equation (1) may be solved for the heat flux.

$$\frac{q}{A_i} = \frac{-\Delta H_v \frac{dm}{dt}}{A_i} \tag{6}$$

Experimentally, values of m, T_{ws}, and T_c are obtained as functions of time during the experimental run. Values for ΔH_v are obtained from published sources and are assumed to be constant. The interfacial area, A_i, is taken as the inner area of the experimental dewar flask.

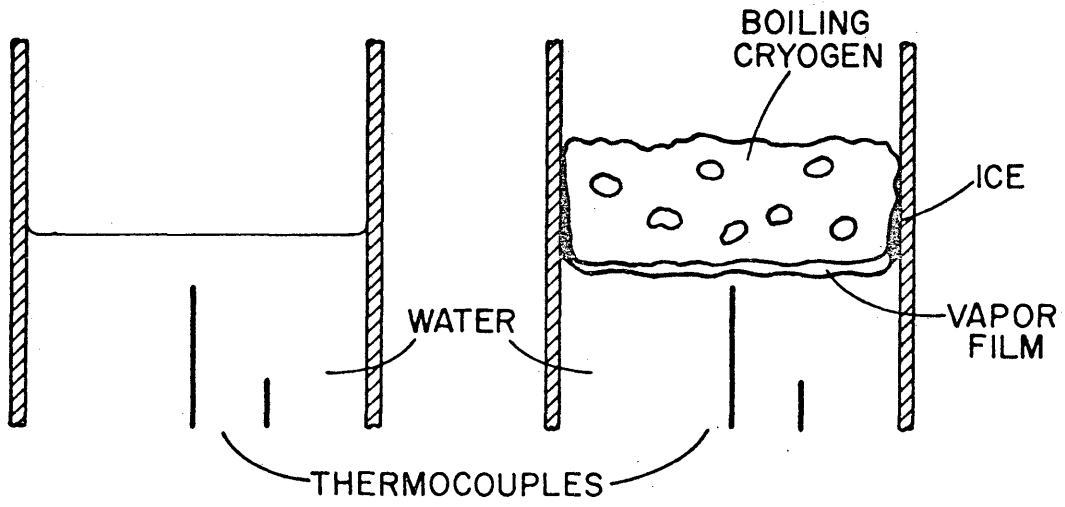

FIGURE 6. DETAILS OF THERMOCOUPLE INSTALLATION IN EXPERIMENTAL DEWAR FLASK

RESULTS

A total of 18 experimental runs were conducted to study film boiling heat transfer between cryogenic liquids and water. Twelve successful experiments were conducted using liquid nitrogen (LN_2), liquid methane gas (LMG), and liquid natural gas (LNG). Attempts to obtain experimental data with liquid ethane gas (LEG) and liquid propane gas (LPG) were unsuccessful.

Experiments were conducted with several points in mind:

1) Study film boiling heat transfer for several cryogenic liquids at the same temperature difference.

2) Study film boiling heat transfer for an individual cryogenic liquid at several different temperature differences.

3) Study the effect of different quantities of cryogenic liquid poured onto the same temperature water surface.

Experimental results will be discussed in detail in the following sections. A general overview of the behavior of each cryogenic liquid will be discussed first.

Liquid Nitrogen (LN_2)

Film boiling heat transfer between LN_2 and water occurs at the largest temperature difference studied. The boiling process was observed to be very stable with no foaming. The interface between the LN_2 and the water was not smooth but rather irregular. Experimental results for the LN_2-water system are tabulated in Tables I-1 to I-6, Appendix I.

Liquid Methane Gas (LMG)

Film boiling between LMG and water was observed to take place with much foaming and bubbling in the LMG phase. During this boiling process, the interface between the LMG and water remained very stable and smooth. Such violent foaming occurred as the LMG was poured onto the water surface that the rate at which the transfer was made took approximately five times longer than for LN_2. Experimental results for the LMG-water system are tabulated in Tables I-7 to I-9, Appendix I.

Liquid Ethane Gas (LEG)

No successful experimental runs were conducted with LEG in three attempts. In each case the LEG-water immediately formed a solid ice-LEG-water block at the interface. Vaporization of the LEG took place and experimental data were recorded although no LEG-water interface was visible. One of the experimental runs is tabulated in Table I-10, Appendix I, for information only.

Liquid Propane Gas (LPG)

No successful experimental runs were conducted with LPG in three attempts. Transfer of the LPG to the water interface resulted in an immediate "pop" with the LPG being blown out of the experimental dewar. In one run, Table I-11, Appendix I, the LPG was very slowly added to the experimental dewar, resulting in the immediate formation of a thin layer of ice. Following the formation of this ice layer, the balance of the LPG was added to the experimental dewar. Data taken in this run represent LPG boiling from an ice surface. Data for this experimental run are attached for information only.

Liquid Natural Gas (LNG)

Three successful experimental runs were conducted with LNG and water. Results of the boiling process were similar to the LMG-water system. If any difference exists, it is in the rate at which ice forms across the water interface. In the LNG-water system, the formation of a continuous ice layer occurred faster than it could be visually recorded. Experimental results for the LNG-water system are tabulated in Tables I-12 to I-14, Appendix I.

Vaporization of the Cryogenic Liquid

The time rate of change of the mass of the cryogenic liquid is one of the principal experimental measurements in this study. A comparison of this variable for LN_2, LMG, and LNG-water systems is shown on Figure 7. The three experimental runs which are compared on Figure 7 will be

used to discuss the important experimental variables. The reason for choosing these particular experimental runs is that a common temperature difference exists which will be used later for other comparisons. The usable data range for each of the experimental runs is indicated on Figure 7. Initial data are not usable because of the initial transient phenomena discussed earlier. The termination of the usable data range was caused by ice forming completely across the interface.

Surface Temperature of the Water Layer

Variation of the surface temperature of the water layer as a function of time is shown on Figure 8 for the three experimental runs being discussed. Initial temperatures of the water layer were chosen to give the same temperature difference between the cryogenic liquid and the water surface. Experimental data show a regular decrease in this surface temperature.

Temperature of the Cryogenic Liquid

Experimental runs conducted with LN_2 and LMG did not exhibit a change in temperature (i. e., boiling point) with time because they are pure materials. Figure 9 shows how the temperature of the boiling LNG increased during the experimental run. This change in boiling point is caused by the lowest boiling point components being distilled off. The rapid temperature increase occurred simultaneously with formation of the ice layer across the water interface. The thermocouple used to measure the boiling cryogenic liquid temperature was contained within the ice layer.

Heat Flux across the Interface

Experimentally determined values of the heat flux across the interface during film boiling between the cryogenic liquids and water are shown on Figures 10-13. Each of these figures will be discussed individually.

Figure 10 compares the interfacial heat flux versus the interfacial temperature difference for the three experimental runs which are being discussed. At a given value of temperature difference, the heat flux increases as the systems change from LN_2-water to LMG-water to LNG-water.

Note also that the heat flux decreases with decreasing temperature difference. This decrease in heat flux occurs as the experimental run proceeds in time because of the cooling of the water surface (see Figure 8).

Figure 11 compares the interfacial heat flux for an LMG-water and an LNG-water system versus the interfacial temperature difference. At a given temperature difference, the LNG-water system has a higher heat flux than the LMG-water system. Heat fluxes for LMG-water and LNG-water systems increased as the interfacial temperature difference decreased. The opposite effect was noted in the LN_2-water system — as the interfacial temperature difference increased, the interfacial heat flux also increased.

Reproducibility of the experimental data for the LN_2-water system is shown on Figure 12. Six experimental runs are shown on this figure. At each of the three temperature levels, two experimental runs were

conducted. The initial quantity of LN_2 poured onto the water surface was varied between the two runs. No effects of the quantity of LN_2 were noted.

A summary of all experimentally determined interfacial heat fluxes as functions of the interfacial temperature difference are shown on Figure 13. Trends of the experimental data are the same as have been discussed previously.

Figure 14 shows a summary of all of the experimentally determined interfacial heat transfer coefficients as functions of the interfacial temperature difference.

Error Analysis

According to Mickley (1957, p. 54), error analysis can be performed as follows. If Q' is a function of several measured quantities, i. e.,

$$Q' = \beta\ (q_1,\ q_2,\ \ldots\ q_n) \tag{7}$$

then the expression for calculating the error in Q' resulting from the measured values is

$$\Delta Q' = \frac{\partial \beta}{\partial q_1}\,\Delta q_1 + \frac{\partial \beta}{\partial q_2}\,\Delta q_2 + \ldots \frac{\partial \beta}{\partial q_n}\,\Delta q_n \tag{8}$$

where the quantities Δq_1, Δq_2, ... Δq_n, are considered as errors in q_1, q_2, ... q_n. This technique often overestimates the error in Q'.

From Equation (2), h_i is given as

$$h_i = \frac{q}{A_i\ \Delta T} \tag{9}$$

Data from Experimental Run No. 12 will be utilized to compute the error in h_i, since this should indicate the maximum error because $q/\Delta T$ will be greatest. In the preceding equation, q is an indirectly determined quantity itself. Equation (1) shows that

$$q = -\Delta H_v \frac{dm}{dt} \tag{10}$$

Approximate values of the data and the estimated maximum errors associated with each variable are taken as:

Variable	Approximate Value	Measured to
ΔH_v	125 cal/g	±6.25 cal/g (5%)
$\frac{dm}{dt}$	−1.75 g/sec	±0.1 g/sec

Partial derivatives of Equation (10) needed for use in an equation of the form of Equation (8) are as follows.

$$\frac{\partial q}{\partial(\Delta H_v)} = -\frac{dm}{dt} \tag{11}$$

$$\frac{\partial q}{\partial \frac{dm}{dt}} = -\Delta H_v \tag{12}$$

Consequently

$$\Delta q = -\frac{dm}{dt}\,\Delta(\Delta H_v) - \Delta H_v\,\Delta\,\frac{dm}{dt} \tag{13}$$

$$\Delta q = +\,1.75\,(6.25) - 125\,(-\,0.1) \tag{14}$$

$$\Delta q = 10.94 + 12.5 = 23.44 \text{ cal/sec} \tag{15}$$

Since the approximate value of q is 218.75 cal/sec, the maximum percentage error is ±(23.44/218.75)100 or ±10.7%.

Returning to Equation (9), the error in h_i for Experimental Run No. 12 can now be estimated.

Variable	Approximate Value	Measured to
q	218.75 cal/sec	±23.44 cal/sec
A_i	16.62 cm^2	±0.4 cm^2
ΔT	200°K	±4°K

Measurement error for A_i was calculated assuming an error in the internal diameter of 0.5 mm. Since each temperature is measured to ±2°K, the maximum possible error of ±4°K was assumed for the temperature difference. Partial derivatives required are

$$\frac{\partial h_i}{\partial q} = \frac{1}{A_i \, \Delta T} \tag{16}$$

$$\frac{\partial h_i}{\partial A_i} = -\frac{q}{A_i^2 \, \Delta T} \tag{17}$$

$$\frac{\partial h_i}{\partial \Delta T} = -\frac{q}{A_i \, \Delta T^2} \tag{18}$$

Consequently

$$\Delta h_i = \frac{1}{A_i \, \Delta T} \Delta q - \frac{q}{A_i^2 \, \Delta T} \Delta A_i - \frac{q}{A_i \, \Delta T^2} \Delta(\Delta T) \tag{19}$$

$$\Delta h_i = \frac{(23.44 \text{ cal/sec})}{(16.62 \text{ cm}^2)(200°\text{K})} - \frac{(218.75 \text{ cal/sec})(-0.4 \text{ cm}^2)}{(16.62 \text{ cm}^2)^2 \, (200°\text{K})}$$

$$- \frac{(218.75 \text{ cal/sec})(-4°\text{K})}{(16.62 \text{ cm}^2)(200°\text{K})^2} \tag{20}$$

$$\Delta h_i = 0.0071 + 0.0003 + 0.0013 = 0.0087 \text{ cal/cm}^2\text{-sec-°K}$$

The approximate value for h_i is 0.0653 cal/cm^2-sec-°K. Therefore, the maximum percentage error is $\pm(0.0087/0.0653)100$ or $\pm 13.3\%$.

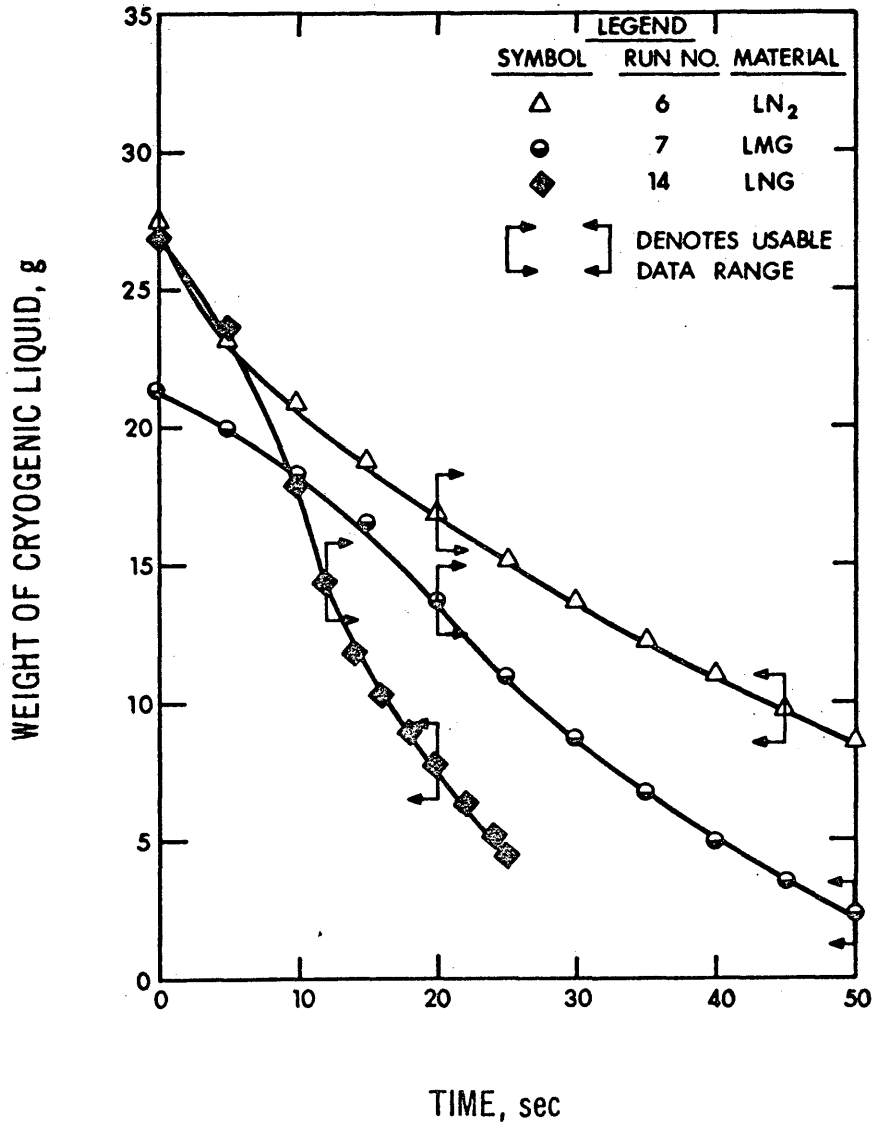

FIGURE 7. CHANGE IN MASS OF THE BOILING CRYOGENIC LIQUID AS A FUNCTION OF TIME

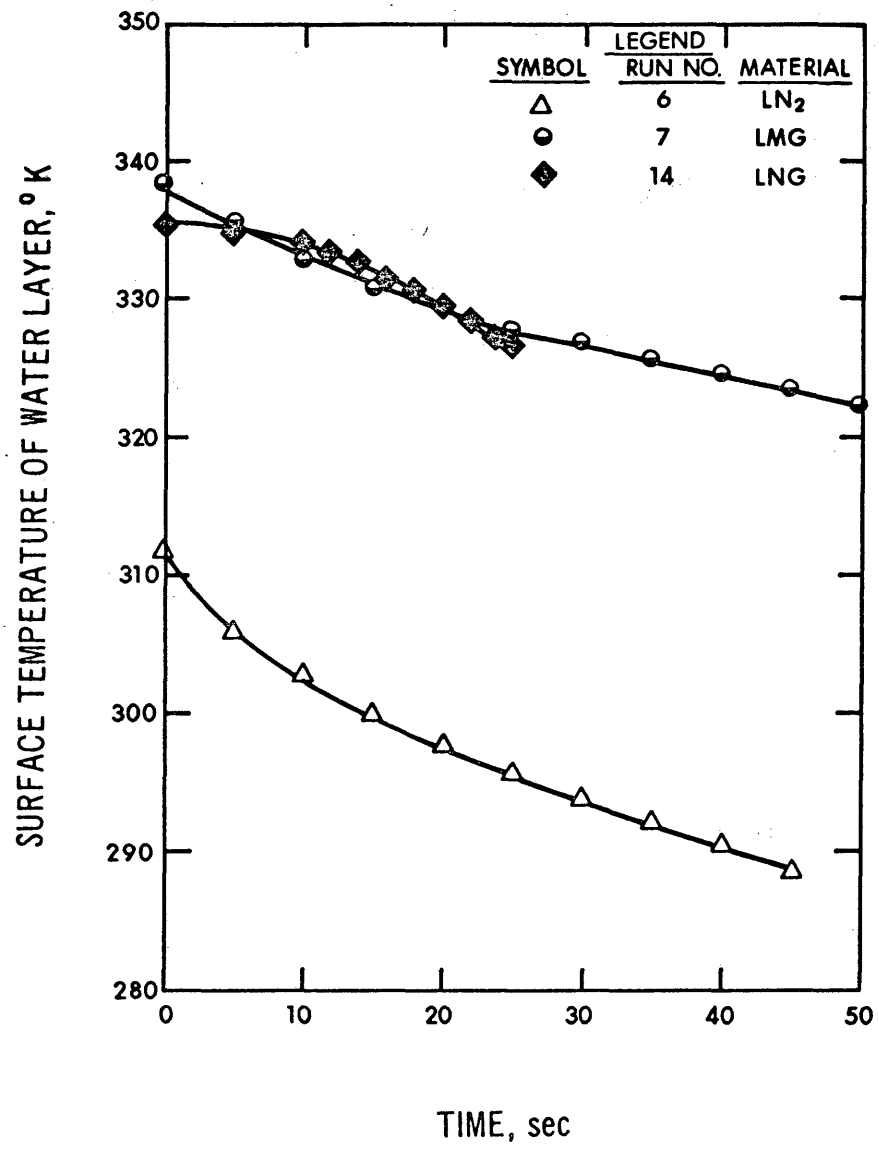

FIGURE 8. CHANGE IN SURFACE TEMPERATURE OF THE WATER LAYER AS A FUNCTION OF TIME

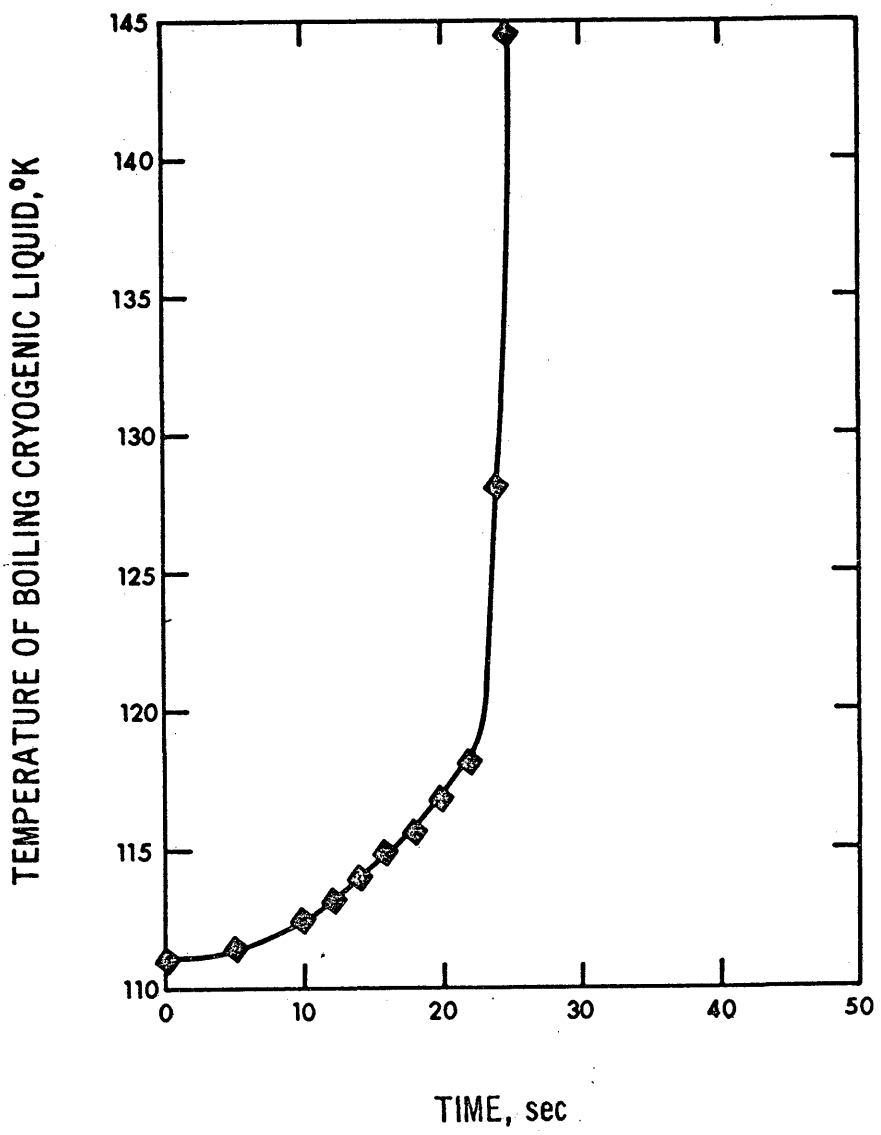

FIGURE 9. CHANGE IN TEMPERATURE OF THE BOILING LIQUEFIED NATURAL GAS AS A FUNCTION OF TIME, EXPERIMENTAL RUN NO. 14

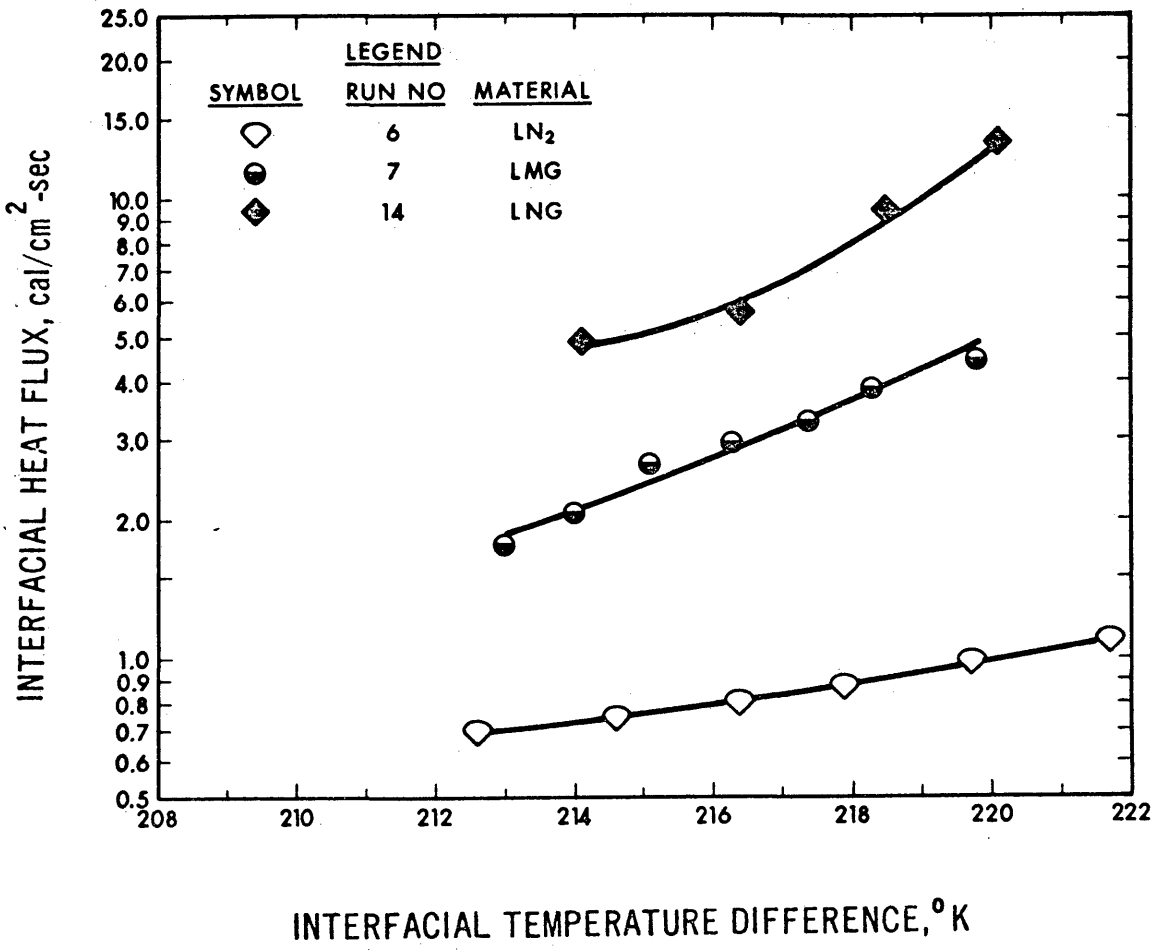

FIGURE 10. COMPARISON OF INTERFACIAL HEAT FLUX AS A FUNCTION OF INTERFACIAL TEMPERATURE DIFFERENCE FOR LN_2-WATER, LMG-WATER, AND LNG-WATER

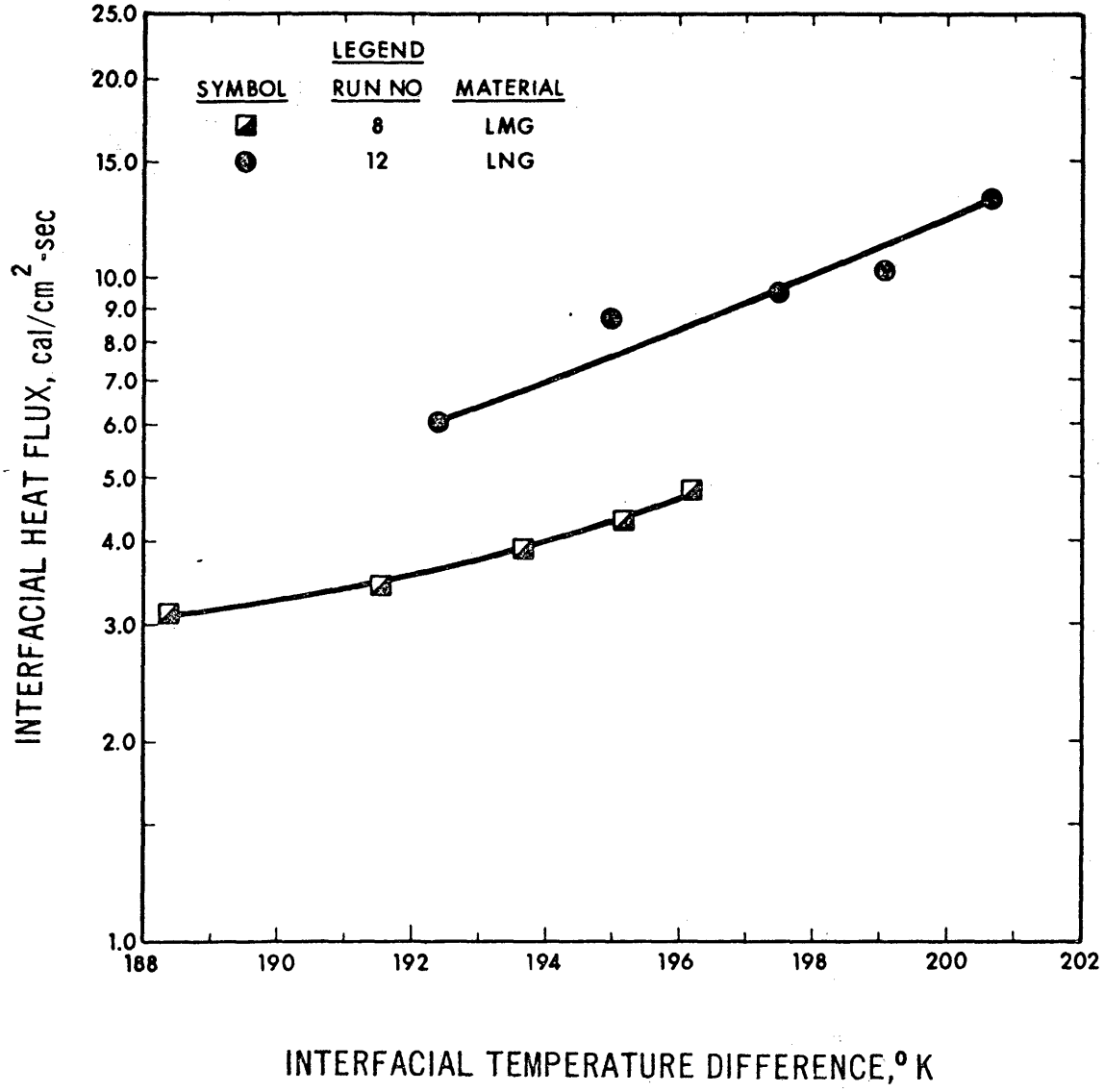

FIGURE 11. COMPARISON OF INTERFACIAL HEAT FLUX AS A FUNCTION OF INTERFACIAL TEMPERATURE DIFFERENCE FOR LMG-WATER AND LNG-WATER

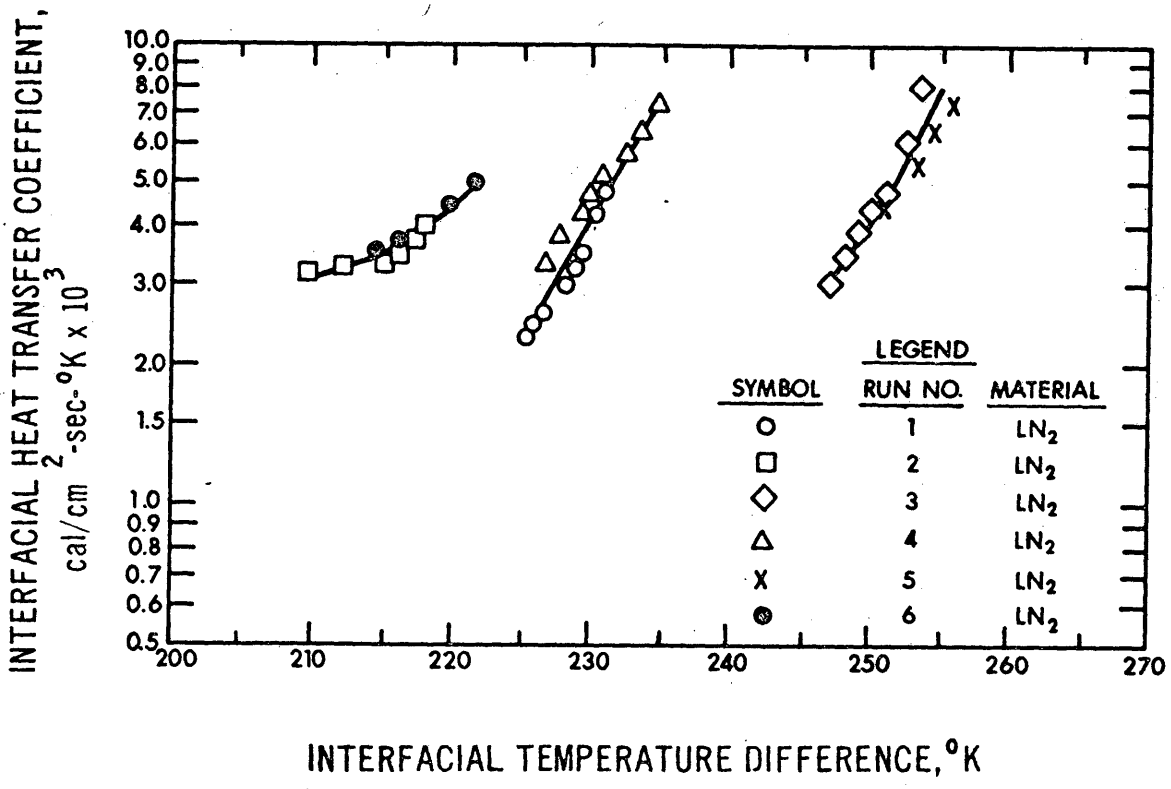

FIGURE 12. REPRODUCIBILITY STUDY OF INTERFACIAL HEAT TRANSFER COEFFICIENT AS A FUNCTION OF INTERFACIAL TEMPERATURE DIFFERENCE FOR THE LN_2-WATER SYSTEM

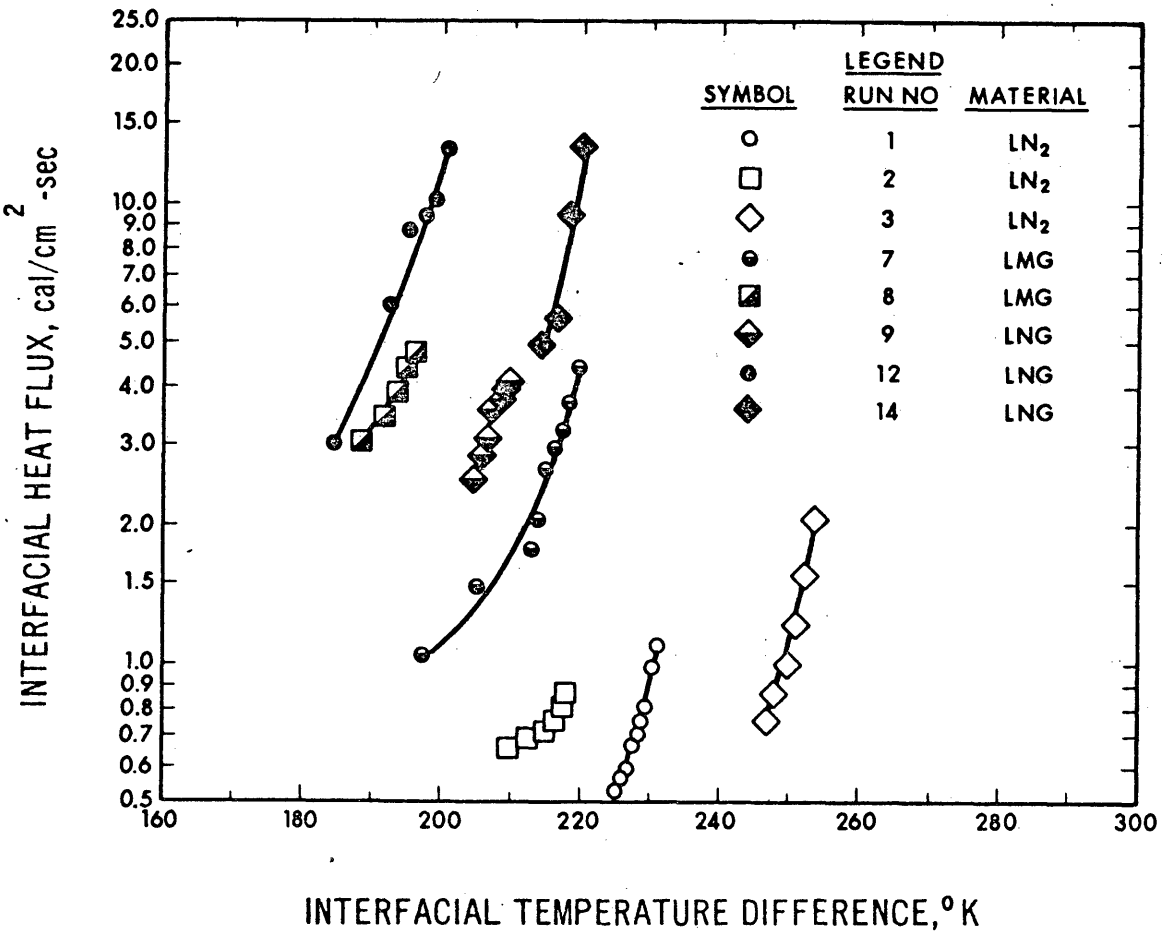

FIGURE 13. EXPERIMENTALLY DETERMINED INTERFACIAL HEAT FLUX AS A FUNCTION OF INTERFACIAL TEMPERATURE DIFFERENCE (NOTE: MULTIPLY THE ORDINATE BY 4.2 TO OBTAIN INTERFACIAL HEAT FLUX IN watts/cm^2 AND BY 13,271 TO CONVERT TO Btu/ft^2-hr)

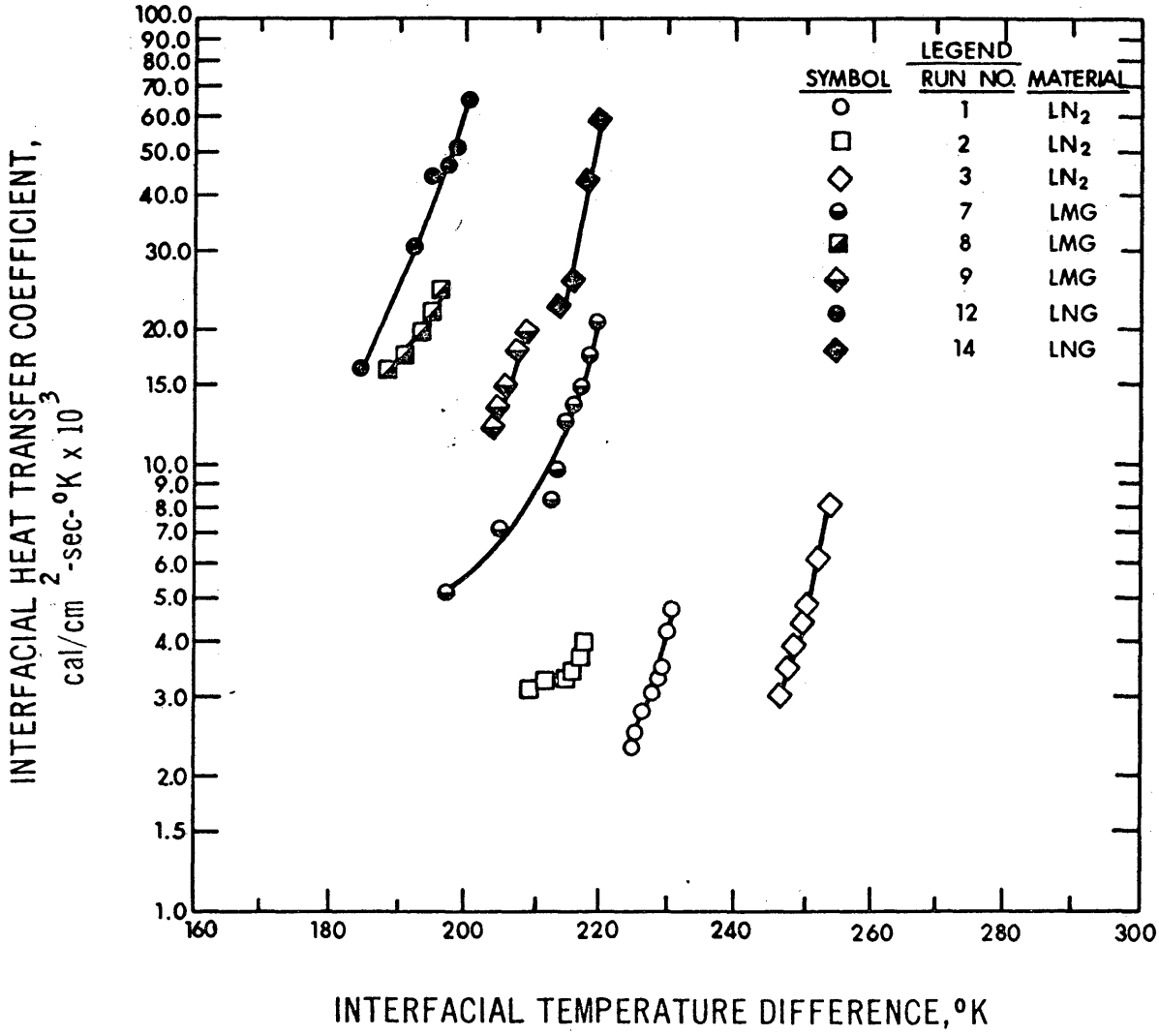

FIGURE 14. EXPERIMENTALLY DETERMINED INTERFACIAL HEAT TRANSFER COEFFICIENT AS A FUNCTION OF INTERFACIAL TEMPERATURE DIFFERENCE (NOTE: MULTIPLY THE ORDINATE BY 4.2 TO OBTAIN INTERFACIAL HEAT TRANSFER COEFFICIENT IN watts/cm^2-°K AND BY 7,373 TO CONVERT TO Btu/ft^2-hr-°F)

DISCUSSION OF RESULTS

Interfacial heat fluxes and interfacial heat transfer coefficients have been determined for film boiling of liquid nitrogen (LN_2), liquid methane gas (LMG), and liquid natural gas (LNG) on water. All experimental data are reported for transient boiling of the cryogenic liquid on a free water surface.

Experiments using liquid ethane gas (LEG) and liquid propane gas (LPG) were unsuccessful. The LEG-water system immediately formed a block of ice completely across the water interface including the cryogenic liquid. The LPG-water system was so unstable that immediately following the transfer of LPG to the water surface, it was blown out of the experimental dewar. It is believed that the LEG and more specifically the LPG boil in the transition region. The transfer of energy in the case of LPG is so fast that the material immediately vaporizes and is propelled out of the experimental dewar flask by its own vapors. In the case of LEG-water, the energy transfer is not fast enough to cause violent vaporization; however, it is sufficiently rapid to immediately cause freezing of the water.

LN_2-Water

Six experimental runs were conducted using the LN_2-water system. Interfacial heat flux and interfacial heat transfer coefficients are shown on Figures 13 and 14. Peak interfacial heat fluxes and interfacial heat transfer coefficients are given in the following table.

TABLE 7

SUMMARY OF LN_2-WATER EXPERIMENTAL RESULTS

Experimental Run No.	Interfacial Temperature Difference, °K	Maximum Heat Flux, cal/cm^2-sec	Maximum Heat Transfer Coefficient, cal/cm^2-sec-°K × 10^3
2	218.0	0.9	4.0
6	221.7	1.1	4.9
1	231.0	1.1	4.7
4	234.8	1.7	7.3
3	253.6	2.1	8.2
5	256.0	1.9	7.4

Errors in the individual experimental runs have been discussed previously. Overall reproducibility of the LN_2-water experimental runs is shown on Figure 12.

Flynn (1961, p. 543) reports film boiling heat flux for LN_2 on a copper heat transfer tube at atmospheric pressure. At a temperature difference of approximately 225°K a heat flux of 0.7 cal/cm^2-sec is reported. Comparison of these data with the experimental data given in Table 7 shows that reasonable agreement is obtained. The difference in atmospheric pressure between the data taken by Flynn at Davenport, Iowa,

and this study conducted at Littleton, Colorado, could explain the small difference. Typically, film boiling of pure compounds from solid surfaces shows that at a given level of heat flux the temperature difference increases as the pressure decreases. In this case, as the pressure increases at a constant temperature difference, the boiling heat flux decreases.

Agreement between the experimental data obtained in this study and that obtained by Burgess and Nakanishi will now be discussed. Burgess (1970, p. 9) reports a maximum boiling heat flux of 1.1 cal/cm^2-sec and an average value of 0.6 cal/cm^2-sec. The interfacial temperature difference is not given. Burgess (1972, p. 14) reports that a value of 0.8 cal/cm^2-sec was obtained in the second phase of testing. Nakanishi (1971b, p. 1) reports experimental data for an interfacial temperature difference of approximately 275°K ranging from 0.7-2.0 cal/cm^2-sec (see Table 2). All of the reported results are in fair agreement with the experimental results obtained in this study.

Nakanishi (1971b, p. 1) reported that following a spill of LN_2 on water at a temperature of 278°K, the temperature 5 mm below the water surface dropped to nearly 105°K after 90 sec. This sudden and drastic lowering of the water temperature was not observed in any of the experimental runs conducted in this study. It is believed that the temperature of an ice layer was actually being measured. Similar results were reported by Burgess (1970, p. 10) and Nakanishi (1971b, p. 2) for LNG-water systems.

A further check of the data in these experimental runs was made by comparing an energy balance on the boiling cryogenic liquid (Equation 1) with an energy balance on the water layer. Three thermocouples located at the surface, 10 mm and 30 mm below the surface of the water layer, are assumed to measure the average temperature of a zone of water. A simple energy balance is then written for each zone and summed to obtain the total energy transferred. After the initial transient boiling period, the energy transferred during a 10-sec time period from the water layer to the boiling cryogenic liquid agreed to within ±5% of the energy balance on the boiling cryogenic liquid.

LMG-Water

Three experimental runs were made using LMG. Interfacial heat flux and interfacial heat transfer coefficients are shown on Figures 13 and 14. Maximum interfacial heat flux and interfacial heat transfer coefficients are shown in the following table.

TABLE 8

SUMMARY OF LMG-WATER EXPERIMENTAL RESULTS

Experimental Run No.	Interfacial Temperature Difference, °K	Maximum Heat Flux, cal/cm^2-sec	Maximum Heat Transfer Coefficient, cal/cm^2-sec-°K $\times 10^3$
8	196.2	4.7	24.1
9	209.7	4.1	19.7
7	219.8	4.4	20.2

Nakanishi (1971b, p. 3) reports similar results for LNG boiling on a water surface at 278°K (see Table 3).

Burgess (1972, p. 15) gives the results shown in Table 5. Effects of different quantities of LMG spilled on water were not included in this study. Burgess reports values for the interfacial heat flux in the range of 1.3-2.7 cal/cm^2-sec. Sciance (1967, p. 400) reports that for LMG film boiling on a gold-plated cylinder at atmospheric pressure and a temperature difference of 200°K, a boiling heat flux of 1.1 cal/cm^2-sec is observed. This value appears to indicate that the work of Burgess was concerned with an LMG-ice system.

LNG-Water

Three experiments were conducted using liquid natural gas (LNG) spilled on water. Table 6 gives an approximate analysis of the LNG used in the spill tests. Summaries of the experimental results are given in Figures 13 and 14. Maximum interfacial heat flux and interfacial heat transfer coefficients are given in the following table.

TABLE 9

SUMMARY OF LNG-WATER EXPERIMENTAL RESULTS

Experimental Run No.	Interfacial Temperature Difference, °K	Maximum Heat Flux, cal/cm^2-sec	Maximum Heat Transfer Coefficient, cal/cm^2-sec-°K $\times 10^3$
13	198.0	12.0	60.8
12	200.7	13.1	65.3
14	220.1	13.1	59.8

During the experimental runs using LNG the temperature of the boiling cryogenic liquid increased during the run because the lowest boiling components were being distilled off. Figure 9 shows an example of this. This observation is not reported by either Burgess or Nakanishi. A detailed examination of data presented by Burgess (1970, p. 10) shows similar data; however, Burgess does not discuss this fact.

Some questions must be raised about the reported data with regard to whether the LNG was boiling on a water surface or on ice. Burgess (1970, p. 5) reported that an ice film formed completely across the water surface between 2 and 3 sec after an LNG spill. Further, Burgess (1970, p. 9) did not obtain significantly different results when LNG was spilled on ice rather than water. An average heat flux of 2.5 ± 0.25 cal/cm^2-sec was reported for all experiments. The water temperature was not reported.

Nakanishi (1971b, p. 2) conducted an experiment using condensed pipeline natural gas (CPG) spilled on a water surface at 353°K and specifically reported that no ice layer was formed. Results of this experiment are shown in Table 2. This table shows an initial boiling heat flux of 5.7 cal/cm^2-sec at the 10-sec point in the experiment dropping to 3.4 cal/cm^2-sec at the 30-sec point.

In this study, Experimental Run No. 14 comes the closest to duplicating the previously discussed experiments. During the time period when the LNG was film boiling on a liquid water surface the interfacial heat flux was experimentally determined to be 13.1 cal/cm^2-sec at an interfacial temperature difference of 220.1°K. Differences between the

results of this study and those of Nakanishi are attributed to two factors:

1) Differences in composition of the LNG used in this study and in the CPG used by Nakanishi (1971a, p. 38). LNG used in this study contained less nitrogen and significantly greater quantities of higher boiling components.

2) Differences in the interfacial temperature difference.

Brown (1968, p. 651) reports film boiling data for LNG using the equipment described by Sciance (1967, p. 396). Temperature differences and experimental pressures were significantly higher than in the present study and no meaningful comparison can be made.

CONCLUSIONS

Experimentally determined interfacial heat fluxes and interfacial heat transfer coefficients as functions of the interfacial temperature difference have been obtained for the film boiling of liquid nitrogen (LN_2), liquid methane gas (LMG), and liquid natural gas (LNG) on water. Experimental results obtained in this study verify other previously published results. It appears that the key variable in the experimental results of this study and the other studies is whether or not the cryogenic liquid is film boiling on a water surface or on an ice surface. Further work is needed to study the formation of ice during the film boiling process.

Accuracy of the experimental results is estimated at ±13.3%. Major contributing factors to the experimental error are the determination of an accurate vaporization rate of the cryogenic liquid and an accurate determination of the area of the water surface once ice formation has started. Temperature measurements are sufficiently accurate; however, the location of the thermocouple measuring the surface temperature of the water is critical. No measurements of the temperature of the vapor

film between the liquids was made. Detailed analysis of the boiling process requires that this temperature must be determined.

Figures 13 and 14 show graphically the experimental results. Neither the interfacial heat flux nor the interfacial heat transfer coefficient is a continuous function of the interfacial temperature difference. This difference may be caused by several factors:

1) inaccurate determination of the water surface temperature

2) inaccurate determination of the area of the water surface

3) contamination of the water surface by the vapor from the boiling cryogenic liquid resulting in changing physical properties. Improvements in the experimental equipment and procedures are needed to clarify this observation.

Because of the widely differing behavior of the LMG-water, LNG-water, LEG-water and LPG-water systems, more composition-dependent studies need to be conducted. Judicious choice of LMG-LEG or LMG-LPG systems may allow experimental studies of the transition boiling region. A refined experimental technique and more sophisticated experimental apparatus will be required to conduct these studies.

The data of this investigation provide a significant extension in the relationship between the interfacial heat flux and the interfacial temperature difference for LN_2, LMG, and LNG film boiling on water. No attempt was made to develop a mathematical correlation for the film boiling process because insufficient data were obtained. Difficulties in obtaining data of the accuracy required for mathematical correlations need to be overcome and more work needs to be undertaken in this area.

NOTATION

A = area, cm^2

ΔH = latent heat of vaporization, cal/g

h = heat transfer coefficient, $cal/cm^2\text{-}sec\text{-}^\circ K$

m = mass, g

q = rate of energy flow across a surface, cal/sec

T = temperature, °K

t = time, sec

Subscripts

c = cryogenic liquid

i = interface

s = surface

v = vapor

w = water

LITERATURE CITED

Brown, L. E., and Colver, C. P., 1967, Nucleate and film boiling heat transfer to a liquefied natural gas, in Advances in cryogenic engineering: New York, Plenum Press, Inc., v. 13, p. 647-654.

Burgess, D. S., Biordi, J., and Murphy, J. N., 1972, Hazards of spillage of LNG into water: PMSRC Report No. 4177, Bureau of Mines, Pittsburgh, Pennsylvania, 86 p.

Burgess, D. S., Murphy, J. N., and Zabetakis, M. G., 1970, Hazards of LNG spillage in marine transportation: SRC Report No. S-4105, Bureau of Mines, Pittsburgh, Pennsylvania, 35 p.

Flynn, T. M., Draper, J. W., and Roos, J. J., 1962, The nucleate and film boiling curve of liquid nitrogen at one atmosphere, in Advances in cryogenic engineering: New York, Plenum Press, Inc., v. 7, p. 539-545.

Mickley, H. S., Sherwood, T. K., and Reed, C. E., 1957, Applied mathematics in chemical engineering: New York, McGraw-Hill Book Co., 413 p.

Nakanishi, E., and Reid, R. C., 1971a, Liquid natural gas-water reactions: Chem. Eng. Prog., v. 67, n. 12, p. 36-41.

——— 1971b, Appendix to LNG-water interactions: Document No. 01622, New York, National Auxiliary Publications Service, 13 p.

Sciance, C. T., Colver, C. P., and Sliepcevich, C. M., 1967, Pool boiling of methane between atmospheric pressure and the critical pressure, in Advances in cryogenic engineering: New York, Plenum Press, Inc., v. 12, p. 395-408.

APPENDIX I

EXPERIMENTAL DATA

TABLE I-1

HEAT TRANSFER DATA, EXPERIMENTAL RUN NO. 1

Initial LN_2 Weight:	20.3 g
Initial LN_2 Temperature:	75.8°K
Initial Water Temperature:	310.0°K
Atmospheric Pressure:	622.8 mm Hg @ 297.4°K

Time, sec	LN_2 Weight, g	Temperature, °K @ Surface	10 mm	30 mm
0.0	20.3	310.0	310.0	310.0
5.0	17.0	308.1	308.6	309.6
10.0*	15.1	306.8	308.1	308.7
15.0	13.4	306.0	307.6	308.2
20.0	12.0	305.2	306.5	307.6
25.0	10.7	304.8	305.8	306.6
30.0	9.5	304.0	305.0	306.1
35.0	8.3	303.4	304.3	305.2
40.0	7.3	302.5	303.4	304.5
45.0	6.3	301.7	302.8	303.8
50.0**	5.4	301.3	302.1	302.9
55.0	4.5	300.7	301.9	302.8
60.0	3.6	300.0	301.4	302.6

TABLE I-2

HEAT TRANSFER DATA, EXPERIMENTAL RUN NO. 2

Initial LN_2 Weight: 16.5 g
Initial LN_2 Temperature: 75.8°K
Initial Water Temperature: 298.3°K
Atmospheric Pressure: 622.8 mm Hg @ 297.5°K

Time, sec	LN_2 Weight, g	Temperature, °K @ Surface	10 mm	30 mm
0.0	16.5	298.3	298.3	298.3
5.0	14.3	295.7	297.0	298.0
10.0*	12.8	293.8	296.8	297.6
15.0	11.4	293.2	296.5	296.8
20.0	10.1	292.0	295.8	296.1
25.0	8.9	291.0	295.2	295.6
30.0	7.7	288.0	294.0	295.0
35.0**	6.5	285.6	293.0	294.6
40.0	5.3	Ice Formed	292.0	293.2
45.0	4.1	Ice Formed	292.0	292.7
50.0	3.3	Ice Formed	291.9	292.4
55.0	2.8	Ice Formed	291.8	292.2
60.0	2.3	Ice Formed	291.8	292.0

TABLE I-3

HEAT TRANSFER DATA, EXPERIMENTAL RUN NO. 3

Initial LN_2 Weight: 25.0 g
Initial LN_2 Temperature: 75.8°K
Initial Water Temperature: 336.4°K
Atmospheric Pressure: 622.9 mm Hg @ 297.5°K

Time, sec	LN_2 Weight, g	Temperature, °K @ Surface	10 mm	30 mm
0.0	25.0	336.4	336.4	336.4
5.0	18.4	330.0	334.0	334.3
10.0*	15.2	329.4	333.0	333.6
15.0	12.5	328.4	332.0	332.5
20.0	10.4	327.0	330.2	330.6
25.0	8.5	325.9	329.0	329.8
30.0	6.8	325.0	327.8	329.0
35.0	5.3	324.0	326.5	327.7
40.0**	4.0	323.0	325.0	326.3
45.0	2.9	322.4	323.8	324.7
50.0	2.0	321.5	322.2	322.9
55.0	1.2	320.5	321.0	322.0
60.0	0.6	319.5	320.5	321.5

TABLE I-4

HEAT TRANSFER DATA, EXPERIMENTAL RUN NO. 4

Initial LN_2 Weight:	31.2 g
Initial LN_2 Temperature:	75.8°K
Initial Water Temperature:	315.5°K
Atmospheric Pressure	623.0 mm Hg @ 297.5°K

Time, sec	LN_2 Weight, g	Temperature, °K @ Surface	10 mm	30 mm
0.0	31.2	315.5	315.5	315.5
5.0	27.4	312.0	313.6	314.0
10.0*	24.4	310.6	311.8	312.6
15.0	22.1	309.5	310.4	311.2
20.0	19.8	308.1	309.9	310.3
25.0	17.7	306.7	308.8	309.4
30.0	15.8	305.8	307.6	308.6
35.0	14.1	305.2	306.5	307.7
40.0	12.6	303.6	305.6	307.1
45.0**	10.3	302.6	304.7	306.1
50.0	9.2	302.2	304.2	305.2
55.0	8.2	301.2	303.7	304.5
60.0	7.3	300.1	303.5	303.8
75.0	4.9	299.0	302.4	302.7
90.0	2.8	297.6	300.2	300.6

TABLE I-5

HEAT TRANSFER DATA, EXPERIMENTAL RUN NO. 5

Initial LN_2 Weight: 33.2 g
Initial LN_2 Temperature: 75.8°K
Initial Water Temperature: 342.0°K
Atmospheric Pressure: 623.2 mm Hg @ 297.3°K

Time, sec	LN_2 Weight, g	Temperature, °K @ Surface	10 mm	30 mm
0.0	33.2	342.0	342.0	342.0
5.0	26.8	334.3	339.5	340.0
10.0	22.7	333.0	338.0	338.3
15.0*	19.4	331.8	336.4	337.0
20.0	16.5	330.5	334.3	335.4
25.0	14.1	329.3	333.0	334.4
30.0	12.0	327.5	332.2	333.6
35.0	10.1	326.8	330.4	332.0
40.0	8.4	325.4	329.2	331.7
45.0	6.7	324.4	328.0	331.3
50.0**	5.4	322.8	326.2	329.8
55.0	4.2	322.2	325.6	329.0
60.0	3.1	320.9	325.2	328.1
75.0	0.5	320.3	324.8	326.7

TABLE I-6

HEAT TRANSFER DATA, EXPERIMENTAL RUN NO. 6

Initial LN_2 Weight: 27.5 g
Initial LN_2 Temperature: 75.8°K
Initial Water Temperature: 311.6°K
Atmospheric Pressure: 622.8 mm Hg @ 296.8°K

Time, sec	LN_2 Weight, g	Temperature, °K @ Surface	10 mm	30 mm
0.0	27.5	311.6	311.6	311.6
5.0	23.1	305.9	308.3	309.4
10.0	20.8	302.8	307.2	309.0
15.0	18.7	299.8	306.1	308.4
20.0*	16.8	297.5	305.1	307.6
25.0	15.1	295.5	303.3	306.1
30.0	13.6	293.7	303.1	304.2
35.0	12.2	292.0	302.9	303.8
40.0	10.9	290.4	302.7	303.2
45.0**	9.7	288.4	302.1	302.8
50.0	8.5	Ice Formed	301.8	302.4
55.0	7.4	Ice Formed	301.6	301.8
60.0	6.3	Ice Formed	301.3	301.4
75.0	3.3	Ice Formed	299.9	300.2
90.0	1.7	Ice Formed	298.3	299.0

TABLE I-7

HEAT TRANSFER DATA, EXPERIMENTAL RUN NO. 7

Initial LMG Weight: 21.3 g
Initial LMG Temperature: 109.4°K
Initial Water Temperature: 338.3°K
Atmospheric Pressure: 623.5 mm Hg @ 298.0°K

Time, sec	LMG Weight, g	Temperature, °K @ Surface	10 mm	30 mm
0.0	21.3	338.3	338.3	338.3
5.0	19.9	335.5	336.8	337.6
10.0	18.2	332.8	336.1	336.8
15.0	16.5	330.7	335.0	336.0
20.0	13.7	329.2	333.9	335.0
25.0*	10.9	327.7	333.3	334.4
30.0	8.7	326.8	332.8	333.2
35.0	6.7	325.7	331.4	332.1
40.0	4.9	324.5	330.8	331.6
45.0	3.5	323.4	330.0	330.6
50.0	2.3	322.4	328.8	329.5
55.0**	1.3	314.9	327.4	328.1
60.0	0.6	306.9	326.5	327.3

TABLE I-8

HEAT TRANSFER DATA, EXPERIMENTAL RUN NO. 8

Initial LMG Weight: 19.8 g
Initial LMG Temperature: 109.4°K
Initial Water Temperature: 309.5°K
Atmospheric Pressure: 623.5 mm Hg @ 298.1°K

Time, sec	LMG Weight, g	Temperature, °K @ Surface	10 mm	30 mm
0.0	19.8	309.5	309.5	309.5
5.0	14.2	306.5	307.8	308.2
10.0*	11.0	305.6	307.3	307.7
15.0	8.1	304.6	306.5	307.3
20.0	5.5	303.1	306.2	307.0
25.0	3.2	301.0	305.5	306.8
30.0**	1.1	297.8	303.9	305.1
35.0	0.0	297.7	302.5	303.3

TABLE I-9

HEAT TRANSFER DATA, EXPERIMENTAL RUN NO. 9

Initial LMG Weight: 19.8 g
Initial LMG Temperature: 109.4°K
Initial Water Temperature: 323.8°K
Atmospheric Pressure: 623.1 mm Hg @ 297.4°K

Time, sec	LMG Weight, g	Temperature, °K @ Surface	10 mm	30 mm
0.0	19.8	323.8	323.8	323.8
5.0	17.1	320.0	322.4	323.0
10.0	14.4	319.1	321.5	321.8
15.0	11.7	318.1	320.8	321.0
20.0*	9.0	317.3	320.2	320.6
25.0	6.5	316.4	319.6	320.0
30.0	4.4	315.8	319.2	319.8
35.0	2.5	315.0	319.0	319.7
40.0**	0.8	314.1	318.0	318.5

TABLE I-10

HEAT TRANSFER DATA, EXPERIMENTAL RUN NO. 10

Initial LEG Weight: 21.2 g
Initial LEG Temperature: 181.0°K
Initial Water Temperature: 301.9°K
Atmospheric Pressure: 623.3 mm Hg @ 297.7°K

Time, sec	LEG Weight, g	Temperature, °K @ Surface	10 mm	30 mm
0.0	21.2	301.9	301.9	301.9
5.0	18.7	299.7	300.8	301.4
10.0	16.2	299.0	300.2	301.1
15.0	14.2	298.3	299.6	300.6
20.0	12.3	297.3	299.3	300.1
25.0	10.5	296.3	298.6	299.9
30.0	8.8	295.1	298.2	299.3
35.0	7.2	294.2	297.4	298.7
40.0	5.7	293.3	296.8	298.0
45.0	4.3	292.3	295.5	297.4
50.0	3.1	291.4	294.8	296.4
55.0	2.1	290.7	294.3	295.7
60.0	1.3	289.9	290.9	294.8

TABLE I-11

HEAT TRANSFER DATA, EXPERIMENTAL RUN NO. 11

Initial LPG Weight: 19.6 g
Initial LPG Temperature: 226.8°K
Initial Water Temperature: 294.0°K
Atmospheric Pressure: 623.7 mm Hg @ 297.9°K

Time, sec	LPG Weight, g	Temperature, °K @ Surface	10 mm	30 mm
0.0	19.6	294.0	294.0	294.0
5.0	16.2	291.2	293.8	294.0
10.0	14.5	286.3	293.1	293.5
20.0	13.2	281.1	292.5	293.0
30.0	11.8	276.5	291.7	292.4
60.0	8.5	270.0	291.0	291.9
75.0	7.3	265.0	290.4	291.2
90.0	6.0	262.4	289.7	290.7
105.0	5.0	260.7	289.3	290.1
120.0	4.0	256.8	288.9	289.8
180.0	0.4	252.0	288.0	289.2

TABLE I-12

HEAT TRANSFER DATA, EXPERIMENTAL RUN NO. 12

Initial LNG Weight: 21.8 g
Initial LNG Temperature: 108.8°K
Initial Water Temperature: 314.5°K
Atmospheric Pressure: 623.8 mm Hg @ 297.7°K

Time, sec	LNG Weight, g	LNG Temperature, °K	Temperature, °K @ Surface	10 mm	30 mm
0.0	21.8	108.8	314.5	314.5	314.5
5.0	19.6	110.5	313.4	314.2	314.4
6.0	17.2	111.1	313.2	314.0	314.3
8.0*	13.7	111.8	312.5	313.6	314.1
10.0	10.0	112.7	311.8	313.2	313.9
12.0	7.5	113.7	311.2	312.8	313.7
14.0	5.2	115.1	310.1	312.4	313.2
16.0	3.6	116.6	309.0	312.0	312.7
18.0**	2.8	123.2	307.8	311.2	311.7
20.0	2.3	156.4	306.5	310.6	311.0

TABLE I-13

HEAT TRANSFER DATA, EXPERIMENTAL RUN NO. 13

Initial LNG Weight:	22.6 g
Initial LNG Temperature:	110.0°K
Initial Water Temperature:	315.5°K
Atmospheric Pressure:	624.0 mm Hg @ 298.0°K

Time, sec	LNG Weight, g	LNG Temperature, °K	Temperature, °K @ Surface	10 mm	30 mm
0.0	22.6	110.0	315.5	315.5	315.5
2.0	20.7	110.6	315.1	315.2	315.3
4.0	18.4	111.2	314.5	314.8	315.0
6.0	15.6	111.9	313.8	314.5	314.7
8.0	12.4	112.7	313.0	314.0	314.5
10.0*	9.2	113.8	311.8	313.7	314.2
12.0	7.6	115.0	310.7	313.3	313.8
14.0	6.7	116.7	309.0	312.9	313.5
15.0**	6.5	120.3	308.6	312.4	313.3

TABLE I-14

HEAT TRANSFER DATA, EXPERIMENTAL RUN NO. 14

Initial LNG Weight: 27.0 g
Initial LNG Temperature: 111.1°K
Initial Water Temperature: 335.6°K
Atmospheric Pressure: 623.9 mm Hg @ 298.3°K

Time, sec	LNG Weight, g	LNG Temperature, °K	Temperature, °K @ Surface	10 mm	30 mm
0.0	27.0	111.1	335.6	335.6	335.6
5.0	23.8	111.6	334.9	334.9	335.2
10.0	17.8	112.4	334.2	334.2	334.2
12.0*	14.3	113.2	333.3	333.4	333.4
14.0	11.8	114.0	332.5	332.6	332.6
16.0	10.3	114.8	331.2	331.5	332.0
18.0**	9.0	115.6	329.7	330.7	331.3
20.0	7.7	116.8	327.6	329.6	330.4
22.0	6.4	118.2	325.0	328.4	329.5
24.0	5.2	128.1	321.9	327.1	328.2
25.0	4.5	144.6	320.3	326.7	327.5

APPENDIX II

ELECTRONIC INSTRUMENTATION DESIGN

ELECTRONIC INSTRUMENTATION DESIGN

In the course of this study it was necessary to design and construct several different electronic instruments in order to obtain the desired levels of stability, sensitivity, and linearity. Detailed descriptions of the major electronic instruments and systems will be given in the following sections. On all electronic schematic diagrams, resistance is given in ohms, Ω, and capacitance is given in microfarads, μf, unless otherwise noted. If not shown, the operational amplifiers use Pin 7 for positive supply voltage (+15v d-c) and Pin 4 for negative supply voltage (−15v d-c).

Thermocouple Amplifier

The thermocouple amplifier is a three-stage amplifier consisting of an input amplifier, an intermediate-stage amplifier, and a buffer amplifier. Figure II-1 is a schematic diagram of the thermocouple amplifier. This amplifier uses μA 725 Instrumentation Operational Amplifiers manufactured by Fairchild Semiconductor, Mountain View, California, in the first two stages, and a Fairchild μA 741 Operational Amplifier in the third stage.

The μA 725 is an instrumentation grade operational amplifier intended for precise, low-level signal amplification applications where low noise, low drift, and accurate closed loop gain are required. Additionally, the offset null capability, high input impedance, and high voltage gain make this device an ideal choice for use in amplifying signals generated by differential thermocouples. The μA 741 is a high performance operational amplifier intended for a wide range of analog applications. High common mode voltage range, short-circuit protection, and absence of "latch-up" tendencies make the μA 741 ideal for use as a buffer amplifier between instrumentation amplifiers and recording devices.

The thermocouple amplifier is designed to provide:

1) Offset null capability for each stage by means of the BALANCE potentiometers. The input to each stage is shorted and the BALANCE potentiometer is adjusted to give 0.000 volt output.

2) Precise gain control for the input amplifier stage by means of the GAIN TRIM potentiometer. This control compensates for the additional resistance caused by ultrafine thermocouple wire.

3) Low gain (10:1) per stage coupled with accurate frequency compensation to maintain linearity.

4) Zero offset adjustment at the input to the intermediate-stage amplifier by means of the ZERO ADJUST potentiometer. A precise 1.000 volt reference voltage is maintained at TP1 and is divided by the ZERO ADJUST potentiometer and summed at the input to the intermediate stage.

By means of this adjustment, different voltages (i. e., temperatures) can be set as the zero point.

5) High frequency noise removal from the input signal via the 0.1 μf capacitor shunted across the negative feedback resistor on each amplifier.

6) Power supply noise removal. This is accomplished by means of the 0.1 μf capacitors located as close to the operational amplifiers as possible.

7) A final matching network to determine the recorder sensitivity. A special resistor, Rg, is included in this network for final adjustment. Details of how the size of resistor Rg is determined are contained in the operating manual for the Honeywell, Series "M" Sub-miniature, Type M40-350A, galvanometers. Factors considered in determining the size of this resistor include the range, sensitivity, and damping factor of the galvanometer.

The thermocouple amplifier has a linearity of ±0.01% and an input sensitivity of ±0.5 microvolt.

Thermocouple Reference Oven

A brass reference oven block maintaining a precise temperature of 35.00 ± 0.02°C is used in this study for the thermocouple reference point. Figure II-2 is a schematic diagram of the reference oven circuit. This circuit uses an LM 308 Precision Operational Amplifier manufactured by National Semiconductor Corporation, Santa Clara, California, in conjunction with a thermistor bridge temperature detector. The LM 308 is a

precision operational amplifier with low input current, low offset voltage, and high input impedance making it specially suited by applications which require long-term stability.

Temperature changes in the brass reference oven block are reflected in resistance changes in the thermistor causing the bridge to become electrically unbalanced. This unbalance then causes the operational amplifier to proportionally drive the power transistors switching voltage to the heating coil.

Special features are used in the construction of the brass reference oven block to insure stability and freedom from electrical noise. The construction sequence is as follows:

1) Wrap the brass block with a single layer of fiberglass tape insulation.

2) Wind the nichrome wire heating element directly onto the insulated brass block spacing it as evenly as possible.

3) Wrap on one layer of fiberglass tape insulation.

4) Wrap this with one layer of aluminum foil for electrostatic shielding.

5) Wrap with several layers ($\sim$1.5 cm) of fiberglass wool insulation.

6) Place in styrofoam container.

Thermocouples are inserted completely through the brass reference oven block, bent back 180°, and reinserted one-half way through to insure thermal tempering. Holes in the oven block are also filled with silicone grease to maintain good heat transfer.

A separate power supply is used for the heater coil to eliminate electrical switching noise as well as to allow better regulation of the voltage supplied to the other instrumentation circuits. Details of this power supply will be discussed later.

Load Cell Signal Conditioner

A signal conditioner is used in conjunction with the load cell weight measurement system. This signal conditioner is used to prevent current loading of the strain gauge bridge circuit in the load cell and thus retain linearity and also amplify the signal for recording on the oscillograph. Figure II-3 is a schematic diagram of the signal conditioner circuit.

Basically, the signal conditioner consists of a buffer amplifier stage to provide a very high input impedance and an amplifier stage to adjust the signal level. LM 308 Precision Operational Amplifiers are used in both stages. Gain adjustment in the amplifier stage provides for a range of 1:1 to 6:1 amplification. A 5 μf capacitor is used to shunt the feedback resistor in the amplifier stage to remove any high frequency noise in the signal.

Long-term stability is insured through the use of the LM 308 Precision Operational Amplifier. The signal conditioner has a linearity of ±0.02% and a sensitivity of ±20 microvolt.

Power Supplies

In order to maintain the stability and accuracy of the electronic instruments used in this study, a Model LXD-3-152 Lambda Precision Power

Supply manufactured by Lambda Electronics Corporation, Melville, New York, was employed. This power supply is regulated to 0.1% accuracy for variations in either line voltage or load current.

A 12v battery and a Fairchild μA 7805 voltage regulator are used to provide 5v d-c to the load cell excitation circuit. A separate power supply not connected to the common ground of the other power supplies or electronic instruments is mandatory for the load cell circuit, or a true differential amplifier is required to sense the output signal. Voltage regulation of 0.1% is maintained by the μA 7805 voltage regulator.

A separate, regulated power supply is used for the heater coil in the thermocouple reference oven circuit. A d-c power supply, Model 6224B, 0-24v, 0-3 amp, manufactured by Hewlett Packard, Palo Alto, California, is used.

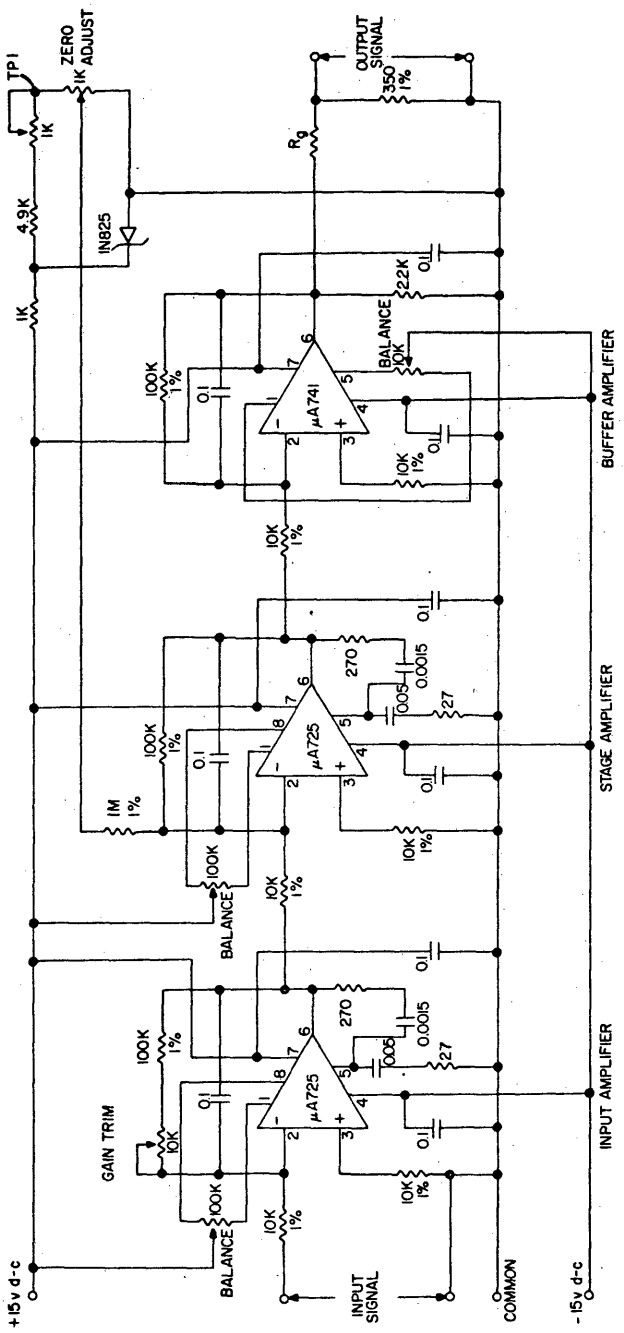

FIGURE II-1. SCHEMATIC DIAGRAM OF THERMOCOUPLE AMPLIFIER

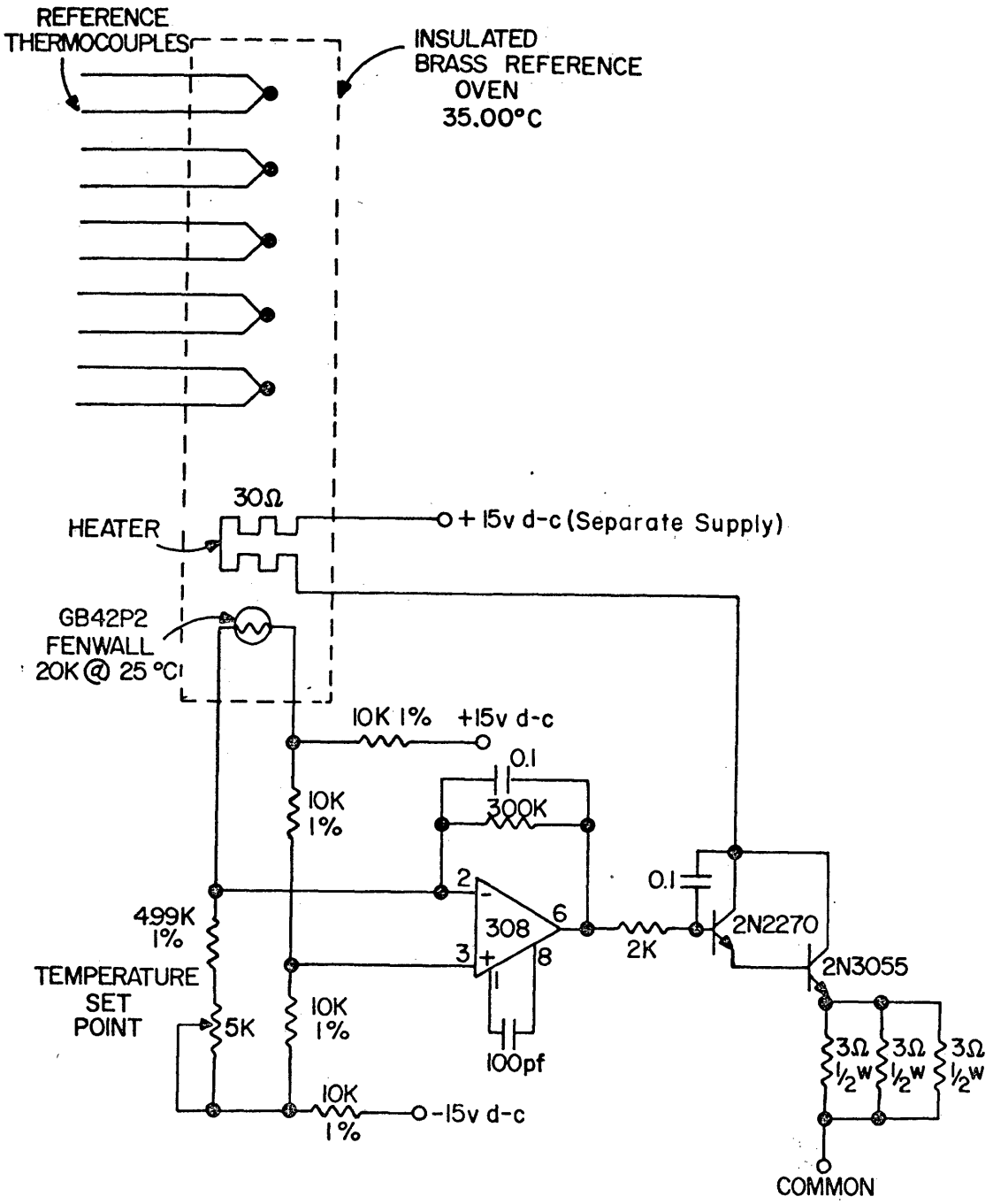

FIGURE II-2. SCHEMATIC DIAGRAM OF THERMOCOUPLE REFERENCE OVEN

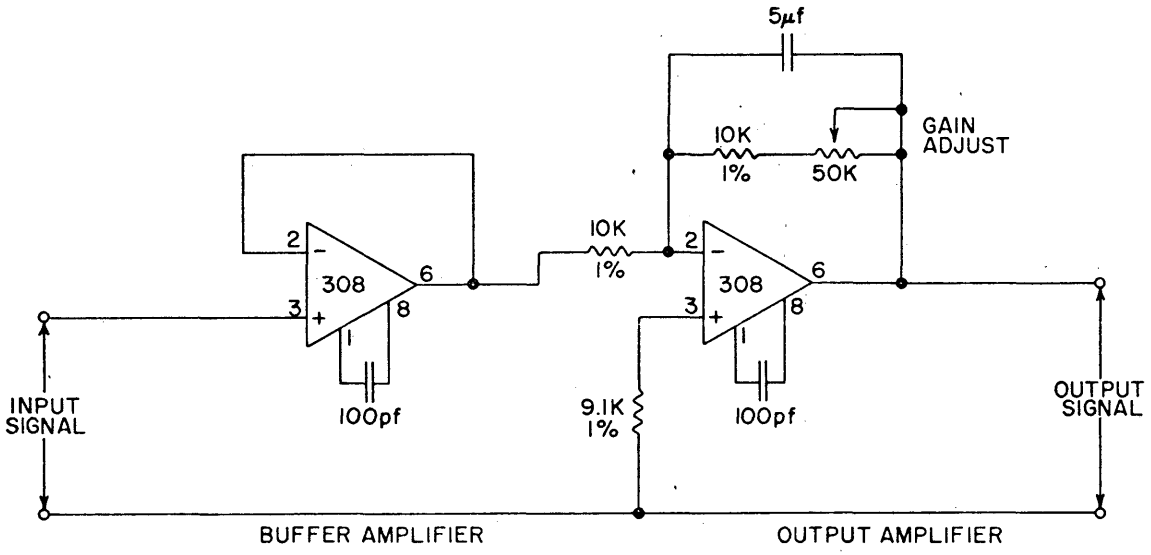

FIGURE II-3. SCHEMATIC DIAGRAM OF SIGNAL CONDITIONER